Quantitative string evolution

C. J. A. P. Martins[*] and E. P. S. Shellard[†]

*Department of Applied Mathematics and Theoretical Physics, University of Cambridge, Silver Street,
Cambridge CB3 9EW, United Kingdom*

An analytic model of long string network evolution, recently developed by the authors, is presented in detail, and modified to describe string loop evolution. By treating the average string velocity, as well as the characteristic length scale, as dynamical variables, one can include the effects of frictional forces on the evolution of the network. This generalized ''one-scale'' model provides a quantitative picture of the complete evolution of a string network, including the prediction of previously unknown transient scaling regimes and a detailed analysis of the evolution of the loop population. The evolution of all cosmologically interesting string networks is studied in detail, and possible consequences of our results are discussed. [S0556-2821(96)05516-6]

PACS number(s): 98.80.Cq, 11.27.+d

I. INTRODUCTION

Symmetry-breaking phase transitions in the early universe inevitably produce topological defects of one form or another. Cosmic strings are of particular interest in this context, unlike some other defects, because the evolution of a string network does not dramatically alter the standard cosmology. In fact, superheavy strings associated with a grand unification phase transition provide a much-studied model for the initial fluctuations for galaxy formation, also leaving imprints in the cosmic microwave radiation background. But cosmological interest in strings is not restricted to grand unified theory (GUT) scales, since strings could have formed at lower energies such as electroweak or Peccei-Quinn symmetry breaking with potentially important consequences, respectively, for baryogenesis or dark matter (axions). Before studying the astrophysical consequences of strings, however, one must know how they are formed and how they evolve. Because of their statistical nature, the best analytic approach consists of doing ''string thermodynamics,'' that is, describing the string network by a small number of averaged quantities.

The serious analytic study of cosmological string networks began one decade ago with Kibble's ''one-scale'' model [1] (later modified by Bennett [2]). In this work it was assumed that the evolution of the long-string network could be described using a single length scale, which is usually called the ''correlation length.'' One then supposes that a scaling solution exists at late times and ends up showing that such a solution will in fact exist and be stable subject to conditions on the loop production mechanisms. Note that in this model it is conceivable that a string network could dominate the energy density of the universe [3].

A step forward in the understanding of string network evolution was provided by numerical simulations (see, for example, [4]). In short, these confirmed the large-scale features of Kibble's model, namely regarding the existence and stability of the scaling solution (at least in the radiation era), but also showed that it neglects important physical processes on small scales. In particular, simulations revealed the existence of a significant amount of small-scale structure on long strings, with loops being predominantly produced at the smallest scales that can be sampled numerically. This change in the understanding of the mechanism of loop formation had of course important consequences, notably in the cosmic string scenario for galaxy and large-scale structure formation.

These findings triggered new efforts on the analytical side to try to account for small-scale structure. Notably, Austin, Copeland, and Kibble developed a model [5] where the evolution of the network is described by three different lengthscales, one of which aims to explicitly describe the presence of small-scale structure. This model also includes a very simple treatment of the effects of gravitational radiation. Apart from confirming the predictions of the one-scale model for the large-scale properties of the network, the main result of this model is the suggestion that the effects of gravitational back-reaction are needed if this ''third lengthscale'' is to reach scaling. A less attractive aspect of this model is that it has to resort to an unappealingly large number of unspecified parameters. There have also been studies of the evolution of the linear kink density in what is effectively a ''one-scale model context'' which anticipated these results by Allen and Caldwell [6] and later by Austin [7].

However, it is usually said that it is very difficult to build a house if one starts with the roof. It is therefore restrictive to try to build models whose only aim is to describe an eventual linear scaling regime. In particular, there is a fundamental ingredient in the evolution of a cosmic string network that has been neglected until very recently, namely frictional forces due to particle-string scattering, which are important for some time after the string-forming phase transition. It should be kept in mind that the period immediately after string formation is by no means irrelevant, e.g., for baryogenesis mechanisms involving cosmic strings. Furthermore, for electroweak strings the friction-dominated epoch only ends in the matter era, lasting almost through to the present day.

A model of string network evolution including the effects

---

*Also at C.A.U.P., Rua do Campo Alegre 823, 4150 Porto, Portugal. Electronic address: C.J.A.P.Martins @ damtp.cam.ac.uk

†Electronic address: E.P.S.Shellard @ damtp.cam.ac.uk

of frictional forces has been recently proposed by the authors [8]. Although it should be seen as the basis for further work, the model is already predictive enough to be testable in both numerical and laboratory experiments, if not cosmologically.

The model is a simple generalization of the "one-scale" model in which the average string rms velocity becomes a dynamical variable. At present, the model does not include small-scale structure (although there are significant hints on how to do it) or other potentially important effects such as loop reconnections onto the long string network. Nevertheless, it will be shown that this simple model provides the first, fully quantitative description of the complete evolution of a string network in the early universe (see Secs. IV and V). In particular, the existence of two different transient scaling regimes in the epoch of friction-dominated dynamics are established (one of which was previously suggested by Kibble). Also, it is apparent in this model that cosmic strings will never dominate the energy density of the universe (for reasons other than the statistical physics arguments of Albrecht and Turok [9]).

Cosmic string loops decay fairly quickly after their formation. For this reason, their contribution to the seeding of gravitational instabilities or cosmic microwave background anisotropies is thought to be subdominant relative to long strings. This fact probably explains why the evolution of the loop distribution has been comparatively neglected in the literature. This gap can be filled by the model to be described here. With simple modifications—the more important of them being the use of the physical loop size ℓ rather then the correlation length L—this model can also be used to study the evolution of the loop distribution. In particular, it will be shown that, depending on the parameters characterizing loop production and lifetimes, there is more energy density in loops than in long strings. Furthermore, the maximum value of the ratio of the loop and background densities occurs shortly after the end of the friction-dominated epoch, and is independent of both the initial conditions and the loop size at formation.

Strings (and topological defects in general), of course, are not exclusive to the early universe. They exist (and have been seen) in a wide variety of condensed matter contexts, including metal crystallization, [10] liquid crystals, [11,12] superfluid helium-3 [13] and helium-4, [14] and superconductivity [15]. Our generalized "one-scale" model can also be used to describe vortex-string evolution in condensed matter contexts (with advantages over previously used approaches). In particular, some well-known results can be readily reproduced, and new quantitative predictions regarding loop production can be made. These issues are discussed in a companion paper [16].

The structure of this paper is as follows. In the next section, after a short review of string dynamics, the evolution equations for the "characteristic lengthscale" and the average velocity of the long string network and each individual loop are derived and justified. The cases of strings arising from the breaking of gauge and global symmetries are both considered. The validity of these "averaged" evolution equations is then tested against simple loop solutions in Sec. III. Section IV contains a discussion on the importance of the friction force in the early universe, together with the analysis of the different scaling laws in the model for both long

strings and loops. There are also some preliminary comparisons with numerical simulations. We then proceed to a detailed and individual analysis of the four physically relevant cases: gauge electroweak and GUT, and global axionic and GUT strings are the subject of Sec. V. Finally, Sec. VI contains conclusions.

Throughout this paper we will use fundamental units in which $\hbar = c = k_B = 1$.

II. A GENERALIZED "ONE-SCALE" MODEL

A. String dynamics with friction

A string sweeps out a two-dimensional surface (the worldsheet) which can be described by spacetime coordinates x^μ and worldsheet coordinates σ^a, $x^\mu = x^\mu(\sigma^a)$; the line element is then

$$ds^2 = g_{\mu\nu} x^\mu_{,a} x^\nu_{,b} d\sigma^a d\sigma^b = \gamma_{ab} d\sigma^a d\sigma^b, \quad (2.1)$$

where $g_{\mu\nu}$ and γ_{ab} are respectively the four-dimensional spacetime and two-dimensional string worldsheet metrics. For the case of a gauge (global) string, one can then derive the Nambu (Kalb-Ramond) action from the Abelian-Higgs (Goldstone) model on the assumption that the scale of perturbations along the string is much larger than its width δ. (In the global case, one also makes use of the equivalence between a real massless scalar field and a two-index antisymmetric tensor field.) One finds

$$S = \mu \int \sqrt{-\gamma} d\sigma^2 \quad \text{gauge}, \quad (2.2)$$

$$S = \mu_0 \int \sqrt{-\gamma} d\sigma^2 + \frac{1}{6} \int \sqrt{-g} H^2 d^4 x$$
$$+ 2\pi\eta \int B_{\mu\nu} d\sigma^{\mu\nu} \quad \text{global}, \quad (2.3)$$

where $B_{\mu\nu}$ is the antisymmetric tensor field, $H_{\mu\nu\lambda}$ is its field strength, and $d\sigma^{\mu\nu}$ is the worldsheet area element. Hence the Nambu action is proportional to the area swept out by the string. By varying this action one obtains the following equations of motion

$$x^\nu_{,a}{}^{;a} + \Gamma^\nu_{\tau\lambda} \gamma^{ab} x^\tau_{,a} x^\lambda_{,b} = 0 \quad \text{gauge}, \quad (2.4)$$

$$x^\nu_{,a}{}^{;a} + \Gamma^\nu_{\tau\lambda} \gamma^{ab} x^\tau_{,a} x^\lambda_{,b} = \frac{2\pi\eta}{\mu_0} H^\nu_{\tau\lambda} \epsilon^{ab} x^\tau_{,a} x^\lambda_{,b} \quad \text{global}. \quad (2.5)$$

It should be noted that in the global case μ_o is the "bare" (unrenormalized) energy per unit length. However, it can be shown that if one distinguishes between the external and self-field contributions to **H** and sets $\mathbf{H}_{\text{self}} = 0$ the above equations still hold with μ_0 replaced by the renormalized energy per unit length, denoted by μ [17].

Still, a crucial ingredient for string evolution is missing. Since strings move through a background radiation fluid, their motion is retarded by particle scattering. Vilenkin has shown [18] that this effect can be described by a frictional force per unit length that can be written

$$\mathbf{F}_f = -\frac{\mu}{\ell_f}\frac{\mathbf{v}}{\sqrt{1-v^2}}, \tag{2.6}$$

where $\mathbf{v}$ is the string velocity and ℓ_f will be called the "friction length scale;" its explicit value depends on the type of symmetry involved. For a gauge string, the main contribution comes from Aharonov-Bohm scattering, [19] while in the global case it comes from Everett scattering [20]. Then we respectively have

$$\ell_f = \frac{\mu}{\beta T^3} \quad \text{gauge}, \tag{2.7}$$

$$\ell_f = \frac{\mu}{\beta T^3}\ln^2(T\delta) \quad \text{global}, \tag{2.8}$$

where T is the background temperature and β is a numerical factor related to the number of particle species interacting with the string (strictly speaking, its value is slightly different in the two cases, but a common symbol will be used for simplicity). Specifically in the gauge case we have

$$\beta = \frac{2\zeta(3)}{\pi^2}\sum_a b_a\sin^2(\pi\nu_a), \tag{2.9}$$

where this sum is taken over effectively massless degrees of freedom, ν_a is the phase change experienced by a particle transported around the string and b_a is 1 for bosons and 3/4 for fermions. Hence Aharonov-Bohm scattering will occur for particles with noninteger $\nu's$; see the paper by Alford and Wilczek in [19] for an example of a model with such values. It should also be noted that the Everett scattering formula is only valid when the particle wavelength is much larger than the string thickness δ.

It is then straightforward to show that the frictional force per unit length (2.6) can be included in the equations of motion (2.4) and (2.5) by adding the term

$$(U^\nu - x_{,a}^\nu x^{\sigma,a}U_\sigma)\frac{1}{\ell_f}, \tag{2.10}$$

(U^ν being the four-velocity of the background fluid) on its right-hand side.

Now consider string motion in an Friedmann-Robertson-Walker (FRW) universe with the line element

$$ds^2 = a^2(\tau)(d\tau^2 - \mathbf{dx}^2); \tag{2.11}$$

then $U^\nu = (a^{-1},\mathbf{0})$ and choosing the gauge conditions $\sigma = \tau$ (i.e., identifying conformal and world sheet times) and $\dot{\mathbf{x}}\cdot\mathbf{x}' = 0$ (i.e., imposing that the string velocity be orthogonal to the string direction) the string equations of motion with the frictional force (2.6) in the background (2.11) can then be expressed as [18,21]

$$\ddot{\mathbf{x}} + \left(2\frac{\dot{a}}{a} + \frac{a}{\ell_f}\right)(1-\dot{\mathbf{x}}^2)\dot{\mathbf{x}} = \frac{1}{\epsilon}\left(\frac{\mathbf{x}'}{\epsilon}\right)', \tag{2.12}$$

$$\dot{\epsilon} + \left(2\frac{\dot{a}}{a} + \frac{a}{\ell_f}\right)\dot{\mathbf{x}}^2\epsilon = 0, \tag{2.13}$$

where the "coordinate energy per unit length" ϵ is defined by

$$\epsilon^2 = \frac{\mathbf{x}'^2}{1-\dot{\mathbf{x}}^2}, \tag{2.14}$$

and dots and primes, respectively, denote derivatives with respect to τ and[1] σ. This form of the evolution equations proves to be particularly useful because dissipation is naturally incorporated in the decay of the coordinate energy density ϵ, while preserving the gauge conditions.

Incidentally, it has been shown [17] that a global string will behave as a superfluid vortex if it is introduced in a homogeneous background of the form

$$H_{\text{ext}}^{ijk} = \sqrt{\rho_h}\epsilon^{ijk} \tag{2.15}$$

(physically, this corresponds to giving it angular momentum). The interaction between this background and the string gives rise to an additional force, known as the (relativistic) Magnus force, and Eq. (2.12) becomes

$$\ddot{\mathbf{x}} + \left(2\frac{\dot{a}}{a} + \frac{a}{\ell_f}\right)(1-\dot{\mathbf{x}}^2)\dot{\mathbf{x}} = \frac{1}{\epsilon}\left(\frac{\mathbf{x}'}{\epsilon}\right)' + \frac{1}{\epsilon}\frac{\rho_h}{\mu}\dot{\mathbf{x}}\wedge\mathbf{m}, \tag{2.16}$$

where

$$\mathbf{m} = \frac{4\pi\eta}{\sqrt{\rho_h}}\mathbf{x}' \tag{2.17}$$

is the circulation vector; the energy equation (2.13) remains unchanged.

B. Lengthscale evolution

We can now proceed to average the string equations of motion to describe the large-scale evolution of the string network. We therefore define the total string energy and the average rms string velocity to be

$$E = \mu a(\tau)\int \epsilon d\sigma, \tag{2.18}$$

$$v^2 \equiv \langle\dot{\mathbf{x}}^2\rangle = \frac{\int\dot{\mathbf{x}}^2\epsilon d\sigma}{\int\epsilon d\sigma}. \tag{2.19}$$

Differentiating Eq. (2.18) and using Eq. (2.13) and (2.19), we see that the total string energy density $\rho \propto E/a^3$ will obey the evolution equation (in terms of physical time t)

$$\frac{d\rho}{dt} + \left(2H(1+v^2) + \frac{v^2}{\ell_f}\right)\rho = 0. \tag{2.20}$$

Equation (2.20) incorporates both long strings and small, short-lived loops which have (in general) a low probability of interacting with other strings before their demise. We shall study the evolution of the long-string network on the

---

[1]Note that reparametrizations of σ can be absorbed into changes of ϵ.

assumption that it can be characterized by a single length scale L; this can be interpreted as the interstring distance or the ''correlation length.'' Strings larger than L will be called long or ''infinite;'' otherwise they will be called loops. For Brownian long strings, we can define the ''correlation length'' L in terms of the network density[2] ρ_∞ as

$$\rho_\infty \equiv \frac{\mu}{L^2}. \qquad (2.21)$$

Following Kibble [1], the rate of loop production from long-string collisions can be estimated as follows. Conceptually, we divide the network into a collection of segments of length L, each in a volume L^3. Consider another segment of length ℓ moving with a velocity v_∞; the probability of it encountering one of the other segments within a time δt is approximately $\ell v_\infty \delta t/L^2$. Consistently with our ''one-scale'' assumption, we then assume that the probability of such an intersection creating a loop of length in the range ℓ to $\ell + d\ell$ will be given by a scale-invariant function $w(\ell/L)$. The rate of energy loss into loops is then given by

$$\left(\frac{d\rho_\infty}{dt} \right)_{\text{to loops}} = \rho_\infty \frac{v_\infty}{L} \int w\left(\frac{\ell}{L} \right) \frac{\ell}{L} \frac{d\ell}{L} \equiv \widetilde{c} v_\infty \frac{\rho_\infty}{L}, \qquad (2.22)$$

where the loop ''chopping'' efficiency $\widetilde{c}$ is assumed to be constant. Note that in previous analyses without friction v_∞ was assumed to be constant and absorbed into the definition of $\widetilde{c}$.

Finally, by subtracting the loop energy losses (2.22) from Eq. (2.20) and then using Eq. (2.21), we obtain the overall evolution equation for the characteristic length scale L:

$$2\frac{dL}{dt} = 2HL(1 + v_\infty^2) + \frac{Lv_\infty^2}{\ell_f} + \widetilde{c} v_\infty. \qquad (2.23)$$

Note that with the exception of the expansion term, all terms on the right-hand side are velocity dependent; this will have important consequences (see below).

C. Loop evolution

On the other hand, we can also study the evolution of the loop density and distribution. The traditional approach is to define $n_\ell(\ell, t)d\ell$ to be the number density of loops with length in the range $(\ell, \ell + d\ell)$ at time t; the corresponding loop energy density distribution is

$$\rho_\ell(\ell, t)d\ell = \mu \ell n_\ell(\ell, t)d\ell. \qquad (2.24)$$

Note that the total loop energy density is

$$\rho_0 \equiv \int \rho_\ell(\ell, t)d\ell, \qquad (2.25)$$

and $\rho = \rho_\infty + \rho_0$.[3] From our assumptions on the loop produc-

tion rate (2.22) it is then easy to see that

$$\frac{d\rho_\ell}{dt} + \left(2H(1 + v_\ell^2) + \frac{v_\ell^2}{\ell_f} \right)\rho_\ell = g\mu \frac{v_\infty \ell}{L^5} w\left(\frac{\ell}{L} \right), \qquad (2.26)$$

where g is a Lorentz factor accounting for the fact that loops are created with nonzero center-of-mass kinetic energy (lost through velocity redshift). However, note that this equation is ''static,'' in the sense that it does not include loop decay mechanisms (e.g., via the emission of gravitational, Goldstone boson, or electromagnetic radiation, as the case may be).

Instead, we start by using our analytic model to describe the evolution of each individual loop. Knowing the energy density transferred from long strings into loops and estimating their sizes at formation (see below), one can numerically determine the energy density in loops and other relevant quantities at all times. This formalism does not allow for loop reconnections, which are unimportant for GUT strings (but can be relevant for high-density electroweak or axionic string networks—see Sec. V); furthermore self-intersections could be included by carefully defining an ''effective'' loop production size.

The physical size of a loop is simply given by

$$\ell = a(\tau) \int_{\text{loop}} \epsilon d\sigma; \qquad (2.27)$$

its time derivative can be easily calculated using (2.13). However one must still subtract energy (hence length) losses due to radiative processes. For the case of a gauge string, this can be roughly estimated from the quadrupole formula

$$\left(\frac{dE}{dt} \right)_{\text{rad}} \sim G\left(\frac{d^3D}{dt^3} \right)^2 \sim G\mu^2 v^6 \qquad (2.28)$$

($D \sim \mu\ell^3$ being the loop's quadrupole moment). Again, note that loop velocity is usually assumed constant ($v_0^2 = 1/2$) and not included in (2.28). (This is obviously correct in the ''free'' regime, but it is not a good assumption in the friction-dominated regime.) Then we define

$$\left(\frac{d\ell}{dt} \right)_{\text{rad}} \equiv -\Gamma' G\mu v^6, \qquad (2.29)$$

where according to numerical estimates $\Gamma' \sim 8 \times 65$ (note that the original parameter Γ was calculated in flat space, where $v_0^2 = 1/2$). Then the evolution equation for the physical loop size has the form

$$\frac{d\ell}{dt} = (1 - 2v_\ell^2)H\ell - \frac{\ell v_\ell^2}{\ell_f} - \Gamma' G\mu v_\ell^6. \qquad (2.30)$$

Again, all but the expansion term are velocity-dependent.

For the case of axionic strings, however, the emission of gravitational radiation is subdominant with respect to the emission of axions. The above expressions will still be valid with the replacement

---

[2]Throughout this paper the subscript ''∞'' refers to properties of the long (''infinite'') string network.

[3]Throughout this paper the subscript 0 refers to properties of the entire loop population; ℓ refers to the loops with length in the range $(\ell, \ell + d\ell)$.

$$\Gamma'G\mu \to q \equiv \frac{\Gamma'}{2\pi}\frac{1}{\ln(\ell/\delta)}, \tag{2.31}$$

where δ is the string thickness. A similar expression also holds for global GUT strings.

Now, we will assume that loop production is "monochromatic," i.e., that loops formed at a time t_p have an initial length

$$\ell(t_p) = \alpha(t_p)L(t_p). \tag{2.32}$$

Notice that we are implicitly saying that the loop size at formation depends both on the large-scale properties of the network (through the correlation length) and on the small-scale structure it contains (through the parameter α). At this stage, since the model does not include small-scale structure, we shall resort to physical arguments about radiative back-reaction, etc., to obtain an *Ansatz* for α when necessary.

With this ansatz the scale-invariant loop production function w [see Eq. (2.22)] becomes

$$w\left(\frac{\ell}{L}\right) = \frac{\widetilde{c}}{\alpha}\delta\left(\frac{\ell}{L} - \alpha\right), \tag{2.33}$$

and the rate of energy loss into loops becomes

$$\left(\frac{d\rho_\infty}{dt}\right)_{\text{to loops}} = g\mu\widetilde{c}\frac{v_\infty}{L^3}, \tag{2.34}$$

with g being the Lorentz factor as above.

Hence the energy density converted into loops from time t to $t+dt$ is

$$d\rho_o(t) = g\mu\widetilde{c}\frac{v_\infty}{L^3}dt; \tag{2.35}$$

this corresponds to a fraction

$$\frac{d\rho_o(t)}{\rho_\infty(t)} = g\widetilde{c}\frac{v_\infty}{L}dt \tag{2.36}$$

of the energy density in the form of long strings at time t. Then using our *Ansatz* (2.33), the corresponding number of loops produced in a volume V is

$$dN(t) = g\frac{\widetilde{c}}{\alpha}\frac{v_\infty}{L^4}V(t)dt; \tag{2.37}$$

hence the ratio of the energy densities in what we will call "dynamic" loops and long strings at time t is

$$\varrho(t)_{\text{dyn}} \equiv \frac{\rho_0(t)_{\text{dyn}}}{\rho_\infty(t)} = gL^2(t)\int_{t_c}^t \frac{dN(t')\ell(t,t')}{V}$$

$$= g\widetilde{c}\,L^2(t)\int_{t_c}^t \frac{a^3(t')}{a^3(t)}\frac{v_\infty(t')}{L^4(t')}\frac{\ell(t,t')}{\alpha(t')}dt', \tag{2.38}$$

where t_c is the moment of the network formation and $\ell(t,t')$ is the length at time t of loops produced at time t'.

Furthermore, we can also find the ratio of the energy densities in "primordial" loops and long strings with a simple modification of our counting strategy: instead of integrating over time, we now integrate over the possible loop lengths in the initial distribution

$$\varrho(t)_{\text{pri}} \equiv \frac{\rho_0(t)_{\text{pri}}}{\rho_\infty(t)}$$

$$= L^2(t)\frac{a^3(t_c)}{a^3(t)}\int_{L_c}^{L_{\text{cut}}} n_\ell(\ell',t_c)\ell(\ell',t_c)d\ell', \tag{2.39}$$

where L_c is the value of the "correlation length" at time t_c, $L_{\text{cut}} \gg L_c$ is a cutoff length, $\ell(\ell',t_c)$ is the length at time t of a (primordial) loop with length ℓ' at t_c, and the loop number density n_ℓ has the well-known Vachaspati-Vilenkin form (see the discussion in Ref. [22]), normalized such that the initial ratio has a value ϱ_c which in this paper we will take (unless otherwise stated) to be $\varrho_c = 0.25$.

We can therefore numerically (and, in some simple limit cases, analytically) determine the loop density at all times. This generalized "one-scale" model can, therefore, provide a complete description of a string network.

D. Velocity evolution

We now consider the evolution of the average string velocity v. A nonrelativistic equation can be easily obtained: it is just Newton's law,

$$\mu\frac{dv}{dt} = \frac{\mu}{R} - \mu v\left(2H + \frac{1}{\ell_f}\right). \tag{2.40}$$

This merely states that curvature accelerates the strings while damping (both from friction and expansion) slows them down. On dimensional grounds, the force per unit length due to curvature should be μ over the curvature radius R. The form of the damping force can be found similarly.

A relativistic generalization of the velocity evolution equation (2.40) can be obtained more rigorously by differentiating Eq. (2.19):

$$\frac{dv}{dt} = (1-v^2)\left[\frac{k}{R} - v\left(2H + \frac{1}{\ell_f}\right)\right]. \tag{2.41}$$

This is exact up to second-order terms. To obtain the damping term we have taken $\langle \dot{\mathbf{x}}^4 \rangle = \langle \dot{\mathbf{x}}^2 \rangle^2$. Writing $\dot{\mathbf{x}}^2 = (1 + \mathbf{p}\cdot\mathbf{q})/2$ (**p** and **p** being unit left- and right-movers along the string) and defining $\mathsf{s} \equiv -\langle \mathbf{p}\cdot\mathbf{q}\rangle$ the difference between the two is

$$\langle \dot{\mathbf{x}}^4 \rangle - \langle \dot{\mathbf{x}}^2 \rangle^2 = \frac{1}{4}[\langle(\mathbf{p}\cdot\mathbf{q})^2\rangle - \mathsf{s}^2]. \tag{2.42}$$

Note that numerical simulations of string evolution indicate that $\mathsf{s}_{\text{rad}} \sim 0.14$ and $\mathsf{s}_{\text{mat}} \sim 0.26$, so this difference should also be small. As for the curvature term, we have introduced R via the definition of the curvature radius vector,

$$\frac{a(\tau)}{R}\hat{\mathbf{u}} = \frac{d^2\mathbf{x}}{ds^2}, \tag{2.43}$$

where $\hat{\mathbf{u}}$ is a unit vector and s is the physical length along the string [related to the coordinate length σ by $ds = |\mathbf{x}'|d\sigma = (1 - \dot{\mathbf{x}}^2)^{1/2}\epsilon d\sigma$]. The dimensionless parameter k is defined by

$$\langle(1-\dot{\mathbf{x}}^2)(\dot{\mathbf{x}}\cdot\hat{\mathbf{u}})\rangle \equiv kv(1-v^2). \qquad (2.44)$$

The parameter k is related to the presence of small-scale structure on strings: on a perfectly smooth string, $\hat{\mathbf{u}}$ and $\dot{\mathbf{x}}$ will be parallel so $k=1$ (up to a second-order term as above), but this need not be so for a wiggly string. On the other hand, $k=0$ for a string loop in flat spacetime—in particular, it is easy (although rather tedious) to show using its definition (2.44) that this is indeed the case for all Kibble-Turok and all Burden loops. In that sense, flat spacetime is the case of maximal small-scale structure; this is not surprising, since there is no mechanism available for kink decay. In a model including small-scale structure, k would probably be a further dynamical variable. For this model, however, we shall use an ansatz interpolating between these two extreme regimes motivated by comparisons with microscopic evolution.

Consider a particular string loop. On large enough scales, they are "frozen" in the background, being conformally stretched by expansion (note that very large loops should only form in friction-dominated regimes). Then they should have relatively little small-scale structure, and taking $k \approx 1$ should be a good assumption. On the other hand, on small enough scales strings behave as if they were in flat spacetime, so one requires that $k \to 0$ as $R \to 0$. In particular, in the case of loops, demanding that their limiting velocity be $v_f^2 = 1/2$ leads to the requirement that $k \propto R$ as $R \to 0$. The remaining point consists in noting that what is dynamically meant by "large" and "small" scales depends not on the relative size of R and the horizon but on the relative size of R and the "damping length" defined as

$$\frac{1}{\ell_d} \equiv 2H + \frac{1}{\ell_f}. \qquad (2.45)$$

With these requirements in mind, and after comparing with the "microscopic" (i.e., unaveraged) evolution of some simple solutions (to be described in the next section) one arrives at the ansatz

$$k = 1, \quad \frac{R}{\ell_d} > \chi, \qquad (2.46)$$

$$k = \frac{1}{\sqrt{2}}\frac{R}{\ell_d}, \quad \frac{R}{\ell_d} < \chi, \qquad (2.47)$$

where χ is a numerical coefficient [23] of order unity. Recall that the physical loop length is approximately $\ell = 2\pi R$; since we will be considering each individual loop, this ansatz applies immediately in that case.

For the case of the long-string network (for which $L = R$), the reasoning is roughly the same in the regime where $L \gg \ell_d$. However, the opposite regime never arises (at least, in the early universe), so there is no simple way of inferring the k behavior. The closest a network gets is in the linear scaling regime in the early universe, where the ratio is

less than, but still of order unity. Of course there is also the problem that k has a slightly different definition—namely, it is an average over the whole network, on a scale of the "correlation length" L. This makes its physical interpretation slightly less clear. For these reasons, when discussing this regime we will start by assuming that k is a constant of order unity. Further justification for this assumption, and a discussion of the possible use of Eq. (2.47) or other alternatives can be found in Sec. IV.

Equations (2.23), (2.30), and (2.41) form the basis of our generalized "one-scale" model, which we will now proceed to apply in several different contexts. We note that the velocity-independent "one-scale" model (2.23) has proved to be successful in describing the large-scale properties of cosmic string networks in numerical simulations. Any deficiencies seem to be associated with the emergence of significant small-scale structure, that is, propagating kinks and wiggles on scales well below L. In friction-dominated regimes, therefore, we should anticipate improved quantitative agreement because of the suppression of this substructure.

III. "AVERAGED" VERSUS "MICROSCOPIC" EVOLUTION

In order to check the validity of our "averaged" evolution model, and in particular our ansatz for k, we will test it against simple loop solutions.

First, consider a circular loop in flat spacetime but with a constant (noninfinite) friction length—i.e., a condensed-matter-like situation. We can describe the loop trajectory simply by

$$\mathbf{x} = r(\tau)(\sin\theta, \cos\theta, 0), \quad \theta \in [0, 2\pi]. \qquad (3.1)$$

Then Eqs. (2.12) and (2.13) reduce to[4]

$$\ddot{r} + (1 - \dot{r}^2)\left(\frac{\dot{r}}{\ell_f} + \frac{1}{r}\right) = 0. \qquad (3.2)$$

Note that the physical ("invariant") loop radius is $R = r/\sqrt{1 - \dot{r}^2}$, obeying

$$\dot{R} = -\dot{r}^2\frac{R}{\ell_f}; \qquad (3.3)$$

also the "microscopic" velocity is $v = -\dot{r}$ and obeys

$$\dot{v} = (1 - v^2)\left(\frac{1}{r} - \frac{v}{\ell_f}\right). \qquad (3.4)$$

On the other hand, our averaged evolution equations (2.30) and (2.41) take the form[5]

$$\frac{d\bar{R}}{dt} = -\bar{v}^2\frac{\bar{R}}{\ell_f}, \qquad (3.5)$$

---

[4]Overdots denote differentiation with respect to conformal time τ, rather than physical time t. In flat space, $\tau = t$.

[5]In this section, averaged quantities will be denoted by overbars.

$$\frac{d\bar{v}}{dt} = (1 - \bar{v}^2)\left(\frac{k(\bar{R})}{\bar{R}} - \frac{\bar{v}}{\ell_f}\right). \tag{3.6}$$

Notice the similarity between the two approaches. Loops with size much larger than the friction length ℓ_f will be overdamped, with the velocity being approximately given by

$$v \sim \frac{\ell_f}{r}. \tag{3.7}$$

In this case the two sets of evolution equations actually coincide—hence justifying our $k = 1$ ansatz for large R. As the loop gains velocity r and R become significantly different and this equivalence ceases to be valid. When R becomes much smaller than ℓ_f, the loop still loses energy due to friction, but this is no longer effective in damping its motion—the loop now begins to oscillate relativistically. In particular, over one ''period'' v oscillates between 0 and 1 (ignoring nonlinear effects near $R = 0$ due to the finite string width). But we know that the averaged velocity should be $\bar{v}^2 = 1/2$ (in the small-scale limit); this is the physical reason why we need k to be a ''phenomenological'' variable. As we mentioned previously, this requirement fixes the behaviour of k on small scales to be as shown in Eq. (2.47). The remaining question is then how to match the two regimes.

First of all, we need a clear idea of when (and where) the transition occurs. A good guess would be the moment of the ''first collapse,'' i.e., the moment when we first have $v = 1$. In fact, this turns out to be a well-defined event. As was first pointed out by Garriga and Sakellariadou [23] [and can be easily seen by analytical or numerical study of the equation of motion (3.2)], circular loops with initial radius much larger than the friction length always reach $v = 1$ for the first time when

$$\left(\frac{R}{\ell_f}\right)_{\text{col}} = \chi_c \simeq 0.569. \tag{3.8}$$

Note that $r_i \gg \ell_f$ is the physically relevant case for string dynamics in condensed matter contexts (recall that the dynamics in that case is always friction-dominated). Also note that because of friction, all loops will rapidly become (almost) circular.

After numerically comparing the averaged and microscopic evolution equations, we find that the simplest possibility (shown in Fig. 1),

$$k = 1, \quad \frac{R}{\ell_f} > \chi_c, \tag{3.9}$$

$$k = \frac{1}{\sqrt{2}} \frac{R}{\ell_f}, \quad \frac{R}{\ell_f} < \chi_c, \tag{3.10}$$

provides excellent agreement for thse circular loops (see Figs. 2 and 3). In particular, this turns out to be significantly better than assuming smoother (and slower) transitions between the two regimes. As can be readily seen, this ansatz provides a very good fit, considering the lack of parameters available.
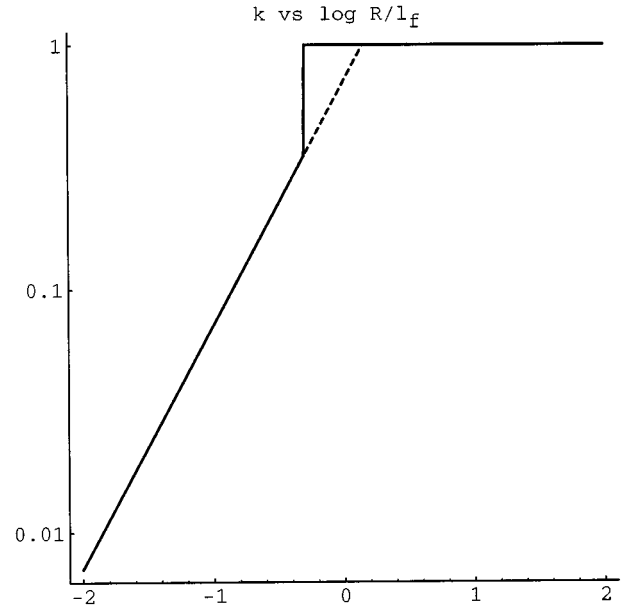

FIG. 1. Two possible *Ansätze* for the parameter k defined in Eq. (2.44), specifically for strings in a condensed-matter context as a function of the rescaled loop radius R/ℓ_f. For the case of string loops, the behavior at large and small scales has a physical justification (see text); numerical matching was improved for circular loops by altering the transition point from $\chi = \sqrt{2}$ (dashed curve) to $\chi \sim 0.57$ (solid curve). However, the *Ansatz* corresponding to the dashed curve might be relevant for long strings (see Sec. IV). The logarithm is to base 10.

In passing, it is worth pointing out that one can also easily calculate the loop lifetime [23]. In the relativistic regime, the $\bar{R}$ evolution equation can be written

$$\frac{d\bar{R}}{dt} = -\frac{\bar{R}}{2\ell_f}, \tag{3.11}$$

so we can immediately estimate that the loop will disappear in a time $t_{\text{dec}} \sim 2\ell_f$ after its first collapse.

The case of the circular loop (3.1) in the expanding universe is analogous, with the constant friction length being replaced by a time-dependent damping length (2.45); also the invariant loop radius is now $R = ar/\sqrt{1 - \dot{r}^2}$. Hence the microscopic evolution equations now take the form

$$\ddot{r} + (1 - \dot{r}^2)\left(a\frac{\dot{r}}{\ell_d} + \frac{1}{r}\right) = 0, \tag{3.12}$$

$$\frac{dv}{dt} = (1 - v^2)\left(\frac{1}{r} - \frac{v}{\ell_d}\right), \tag{3.13}$$

$$\frac{dR}{dt} = HR - v^2\frac{R}{\ell_d}. \tag{3.14}$$

Neglecting the gravitational radiation term (whose form has been established elsewhere), the averaged evolution equations are
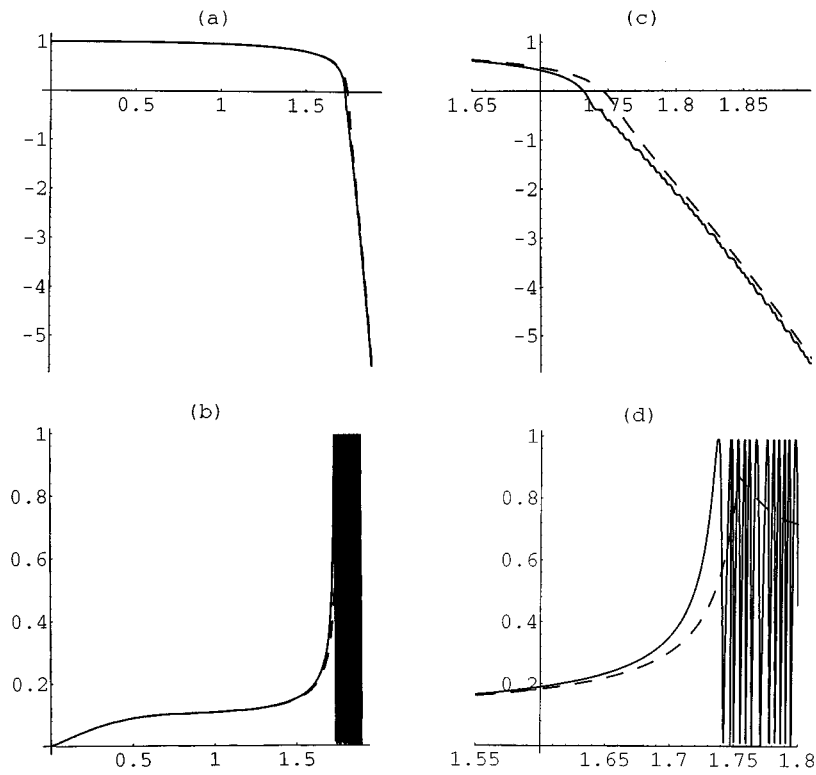
FIG. 2. Comparing the ''microscopic'' (solid lines) and ''averaged'' (dashed) evolution equations for a circular loop in a condensed-matter context. Length and time are in units of ℓ_f, and the time axis is with a logarithmic scale. Plot (a) depicts the log of the (rescaled) radius, while (b) depicts the loop velocity. (c) and (d) are close-ups of (a) and (b), respectively.
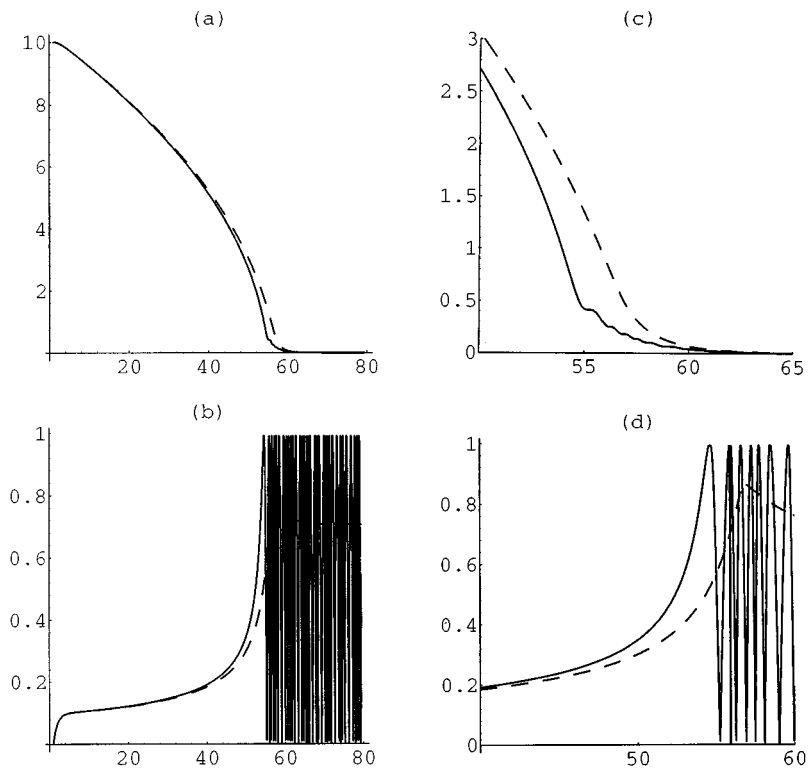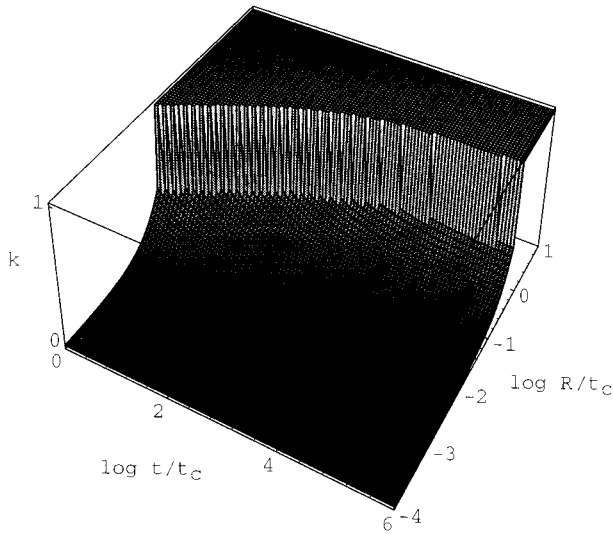

FIG. 3. Comparing the ''microscopic'' (solid lines) and ''averaged'' (dashed) evolution equations for a circular loop in a condensed-matter context. Length and time are in units of ℓ_f, and the time axis is with a linear scale. Plot (a) depicts the log of the (rescaled) radius, while (b) depicts the loop velocity. (c) and (d) are close-ups of (a) and (b), respectively.

FIG. 4. The ansatz for parameter k for gauge GUT string loops, as a function of loop radius and time after the formation of the string network (see Sec. V). The logarithm is to base 10.

$$\frac{d\bar{R}}{dt} = (1 - 2\bar{v}^2)H\bar{R} - \bar{v}^2\frac{\bar{R}}{\ell_f}, \tag{3.15}$$

$$\frac{d\bar{v}}{dt} = (1 - \bar{v}^2)\left(\frac{k(\bar{R})}{\bar{R}} - \frac{\bar{v}}{\ell_d}\right). \tag{3.16}$$

Corresponding to this change, we simply modify ℓ_f to ℓ_d in our ansatz for k, which becomes Eq. (2.47) (see Figs. 4 and 5). However, the numerical value of the ratio of R and ℓ_d when the loop first collapses, χ, is now slightly smaller:

$$\chi = 0.431 \quad \text{radiation}, \tag{3.17}$$

$$\chi = 0.380 \quad \text{matter}. \tag{3.18}$$
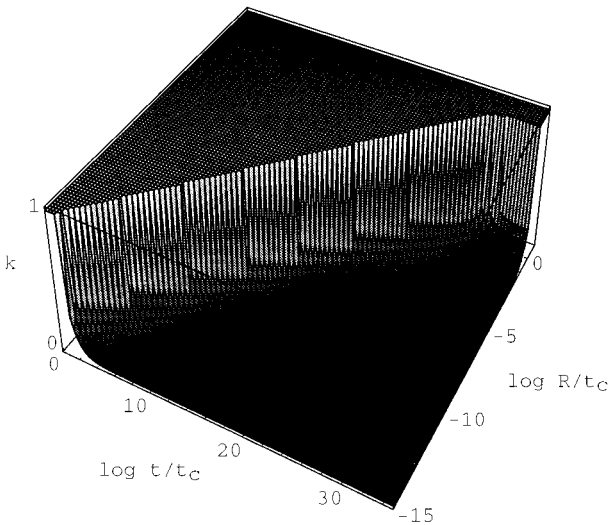
FIG. 5. The *Ansatz* for parameter k for gauge electroweak string loops (compare with Fig. 4). Note that these units $t_{eq} \sim 22.1$, friction ceases to dominate the dynamics at $t_* \sim 25.8$, and the present time is $t_o \sim 28.5$. The logarithm is to base 10.

Numerically we find that a slightly larger value, $\chi \sim 0.5$ provides the best fit in both cases. It is also interesting to note that while the radiation-era evolution is rather insensitive to the value of χ (in the range $\chi \sim 0.3-0.6$ say), the matter-era evolution exhibits a stronger dependence.

Figures 6 and 7 depict the evolution of a loop with initial radius $R_i = 10t_i$ in the radiation $(t_i = t_c)$ and matter $(t_i = t_{eq})$ eras—see Sec. IV. Again, the loops are initially overcritically damped, the approximate velocity being

$$v \sim \frac{\ell_d}{R}. \tag{3.19}$$

The effect of damping is essentially twofold. Firstly, it delays the moment when the loop first collapses. While its velocity is nonrelativistic, there is no loss of length through velocity redshift [see Eq. (3.15)], and so the physical loop radius can grow to a size much larger than the initial radius. As it picks up speed, however, it starts losing more energy. As we mentioned above, the first collapse still occurs for $R \sim \ell_d$; in the relativistic regime, the loop loses energy at each oscillation as before.

Finally, when friction has switched off (and the period of oscillation is much shorter than the expansion rate) the loop starts to oscillate with constant physical amplitude [see (3.15)]. Notice that due to the additional effect of friction this energy loss is much larger in the radiation era. In our case, in the radiation era the "final" physical radius is almost equal to the initial radius, whereas in the matter era it is more than one order of magnitude larger. When this final stage is reached, gravitational radiation or other preferred decay channels cause the loop to shrink further.

Having thus established, in simple but physically relevant cases, the validity of our generalized "one-scale model," and in particular of the ansatz for k, we now proceed to apply it to the study of cosmic string evolution; the study of string evolution in condensed matter contexts is left for a companion paper [16].

IV. GENERAL SCALING RESULTS

A. Introduction

In the early universe the friction lengthscale increases with time, so friction will only be important at early times [23]; however, the meaning of "early" is, as we will see, model-dependent. Again let T_c be the temperature of the string-forming phase transition; the corresponding time of formation is

$$t_c = \frac{1}{f}\frac{m_{Pl}}{T_c^2}, \tag{4.1}$$

where f is given by

$$f = 4\pi\left(\frac{\pi\mathcal{N}}{45}\right)^{1/2}, \tag{4.2}$$

and $\mathcal{N}$ is the number of effectively massless degrees of freedom in the model (e.g., $\mathcal{N} = 106.75$ for a minimal GUT model, but it can be as high as 10^4 for particular extensions
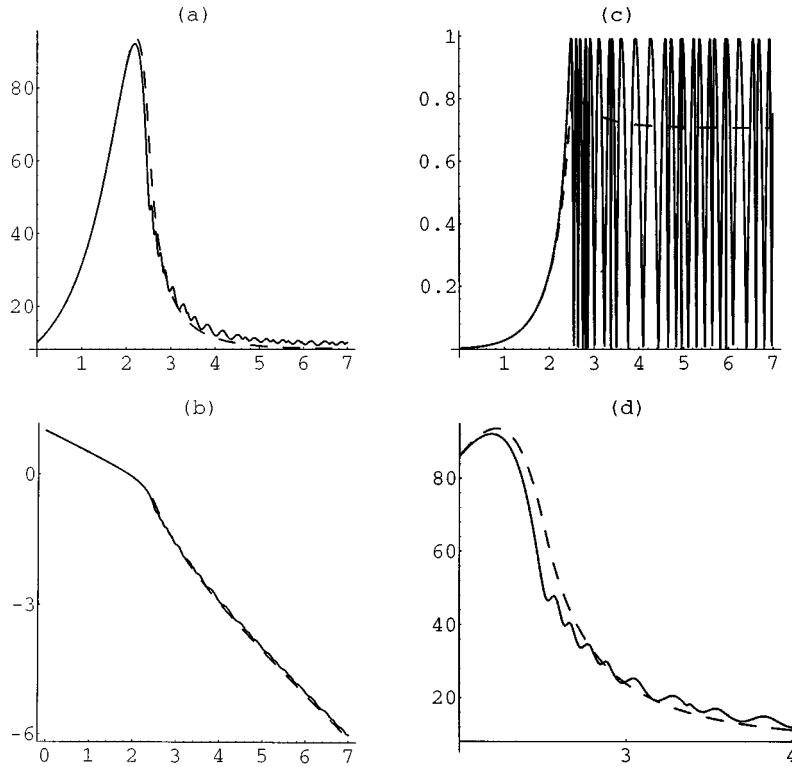
FIG. 6. Comparing the ''microscopic'' (solid) and ''averaged'' (dashed) evolution equations for the physical radius (a), the log of the radius relative to the horizon (b), and velocity (c) of a circular gauge GUT loop formed at $t = t_c$ with radius $R = 10 t_c$; (d) is a closeup of (a). Time is in orders of magnitude from the moment of loop formation. Radiative mechanisms are not included.

of it). Then in the case of a gauge symmetry breaking the friction lengthscale can be written

$$\ell_f = \frac{1}{\theta} \frac{t^{3/2}}{t_c^{1/2}} \quad \text{radiation,} \tag{4.3}$$

$$\ell_f = \left(\frac{3}{4} \right)^{3/2} \frac{1}{\theta} \frac{t^2}{(t_c t_{\text{eq}})^{1/2}} \quad \text{matter,} \tag{4.4}$$

and for the case of a global symmetry

$$\ell_f = \frac{1}{4\theta} \frac{t^{3/2}}{t_c^{1/2}} \ln\left(\frac{L}{\delta} \right) \left[\ln\left(\frac{6}{\lambda} \frac{t_c}{t} \right) \right]^2 \quad \text{radiation,} \tag{4.5}$$

$$\ell_f = \left(\frac{3}{4} \right)^{3/2} \frac{1}{4\theta} \frac{t^2}{(t_c t_{\text{eq}})^{1/2}} \ln\left(\frac{L}{\delta} \right) \left[\ln\left(\frac{8}{\lambda} \frac{t_c t_{\text{eq}}^{1/3}}{t^{4/3}} \right) \right]^2 \quad \text{matter.} \tag{4.6}$$

The constant θ is a measure of the importance of the friction term in the evolution equations; its value is

$$\theta = \frac{\beta}{\sqrt{f}} \left(\frac{t_c}{t_{\text{Pl}}} \right)^{1/2}. \tag{4.7}$$

Note that as we mentioned previously, β is not exactly the same in the gauge and global cases. Also, Eq. (4.3) is valid almost immediately after t_c (so we will begin studying the evolution of the network at $t_i \approx t_c$), but Eq. (4.5) is only valid for $t/t_c > 6/\lambda$. The string energy per unit length can again be written

$$\mu = T_c^2 \quad \text{gauge,} \tag{4.8}$$

$$\mu = T_c^2 \ln\left(\frac{L}{\delta} \right) \quad \text{global.} \tag{4.9}$$

Defining t_* as the time at which the two damping terms in Eqs. (2.12) and (2.13) have equal magnitude we find

$$\frac{t_*}{t_c} = \theta^2 \quad \text{gauge,} \tag{4.10}$$

$$\frac{t_*}{t_c} = 16\theta^2 \left(\ln\frac{L}{\delta} \right)^{-2} \left[\ln\left(\frac{6}{\lambda} \frac{t_c}{t_\star} \right) \right]^{-4} \quad \text{global,} \tag{4.11}$$

provided this is still in the radiation era; otherwise, in the matter era we obtain

$$\frac{t_*}{t_c} = \left(\frac{4}{3} \right)^{1/2} \theta \left(\frac{t_{\text{eq}}}{t_c} \right)^{1/2} \quad \text{gauge,} \tag{4.12}$$

$$\frac{t_*}{t_c} = 4 \left(\frac{4}{3} \right)^{1/2} \theta \left(\frac{t_{\text{eq}}}{t_c} \right)^{1/2} \left(\ln\frac{L}{\delta} \right)^{-1}$$

$$\times \left[\ln\left\{ \frac{8}{\lambda} \left(\frac{t_{\text{eq}}}{t_c} \right)^{1/3} \left(\frac{t_c}{t_\star} \right)^{4/3} \right\} \right]^{-2} \quad \text{global.} \tag{4.13}$$

String dynamics is friction dominated from t_c until t_*, after which motion will become relativistic or ''free.'' A simple heuristic argument (see, for example, [24]) due to Kibble suggests that in the damped phase the correlation length will
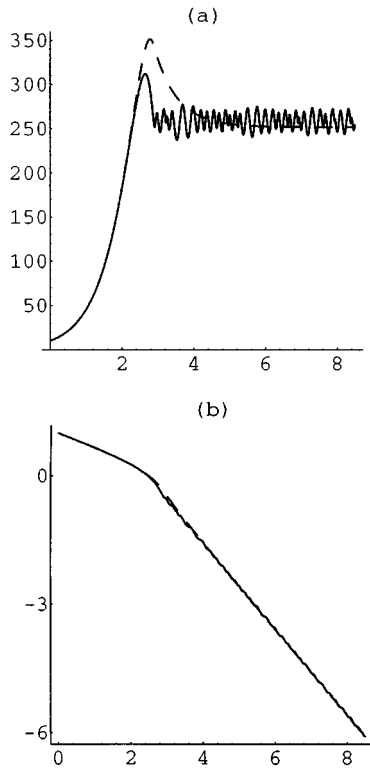
FIG. 7. Comparing the ''microscopic'' (solid) and ''averaged'' (dashed) evolution equations for the physical radius (a) and the log of the radius relative to the horizon (b) of a circular gauge GUT loop formed at $t = t_{eq}$ with radius $R = 10t_{eq}$. Time is in orders of magnitude from the moment of loop formation. Radiative mechanisms are not included.

scale as $L \propto t^{5/4}$; it is worth noting that this argument is rather similar to the ones used in condensed-matter contexts.

We now address the problem of initial conditions. Starting with the correlation length, by causality this must obviously be smaller than the horizon; but on the other hand, it must be greater than the friction length scale since friction is initially dominating the dynamics. We will therefore assume (following [24]) that

$$\ell_{fi} < L_i < t_i. \tag{4.14}$$

For simplicity, we now concentrate on the gauge case, and define $\widetilde{L} \equiv L/t_c$. Then Eq. (4.14) can be written

$$\theta^{-1} < \widetilde{L}_i < 1; \tag{4.15}$$

these two extreme limits could correspond to a rapid second-order phase transition ($\widetilde{L}_i \sim \theta^{-1}$) or a slow first-order transition ($\widetilde{L}_i \sim 1$). Now, the parameter β in Eq. (2.9) can be written

$$\beta = \frac{2\zeta(3)}{\pi^2} \mathcal{N}\omega, \tag{4.16}$$

(where $0 \leq \omega < 1$) and using the definitions of θ and f, one finds that the initial ratio of the string and background densities obeys

$$\frac{32\pi}{3} G\mu \leq \left(\frac{\rho_\infty}{\rho_b} \right)_i \leq \frac{60\zeta(3)}{\pi^4} \omega(\leq 0.75). \tag{4.17}$$

In fact, by analyzing the evolution equations (2.23) and (2.41) one can show that for all physically reasonable values of $\widetilde{c}$ and k these bounds hold for all subsequent times. Consequently, cosmic strings can never dominate the universe. It can analogously be shown that this is also true in the case of a global symmetry, although the required algebra is slightly more complicated. Note that this is an entirely different (and independent) argument to the Albrecht-Turok [9] statistical physics argument—in a sense, it is a ''thermodynamical'' argument.

As for the initial velocity, it can be estimated by a very simple (and rough) argument. The friction lengthscale can be approximately interpreted as the distance that a piece of string can travel before it is stopped by the friction force. Then by comparing the energy contained in strings in a volume L^3 and the work done by the friction force in stopping them we obtain

$$\mu L_i \sim \frac{\mu v_i}{\ell_{f_i}} L_i^2, \tag{4.18}$$

and substitution of ℓ_f yields

$$v_i \left(\frac{L}{t} \right)_i \sim \left(f \frac{t_{Pl}}{t_c} \right)^{1/2}. \tag{4.19}$$

As expected, highly-curved strings will have high velocities and conversely strings in low-density networks will have small velocities.

B. Long-string scaling laws

Analysis of the evolution equations for the correlation length and velocity of the long string network Eqs. (2.23) and (2.41) reveals the existence of three types of scaling regimes, which we now describe in detail. Two of these regimes are transient, occurring in the friction-dominated epoch. In this situation strings should have very little small-scale structure, and we should have $k = 1$. In analogy with our discussion for string loops in Sec. III, we should also find that the string velocity in the radiation era is

$$v \propto \frac{\ell_d}{L}, \tag{4.20}$$

which is in fact the case (see below). The third is the well-known linear scaling regime.

Recall that t_c [defined in Eq. (4.1)] denotes the time of string formation; on the other hand, t_s will denote the time at which the relevant period of evolution starts.

1. Stretching regime

This is a transient regime that occurs in the beginning of the friction-dominated phase, provided the initial string density is sufficiently low. With $t_s = t_c$ we get

$$L = L_s \left(\frac{t}{t_s} \right)^{1/2}, \tag{4.21}$$

$$v = \frac{t}{\theta L_s} \quad \text{gauge,} \tag{4.22}$$

$$v = \frac{t}{\theta L_s} \left[\ln\left(\frac{\lambda}{6} \frac{t}{t_s}\right) \right]^2 \ln\frac{L}{\delta} \quad \text{global.} \tag{4.23}$$

The reason why this regime arises is physically obvious. If we start with a small string density, the correlation length will be close to the horizon, and much larger than the damping length. Hence long strings are fairly straight and have very little small-scale structure. This is therefore analogous to the situation in condensed matter—the strings have very small velocities and are ''frozen,'' being conformally stretched by the expansion.

Mathematically, the $L \propto t^{1/2}$ law comes immediately from the fact that the friction, loop production and redshift terms in the evolution equation for L are all velocity dependent, and can therefore be neglected when compared to expansion. Note, however, that unlike the condensed matter case there is no additional logarithmic correction to the $L \propto t^{1/2}$ law in the case of a global string network. Finally, and although this is not cosmologically relevant, it should be pointed out that the corresponding regime in the matter era would be

$$L \propto t^{2/3}, \quad v \propto t^{4/3}. \tag{4.24}$$

2. Kibble regime

This is a transient regime that also occurs in the friction-dominated epoch (following the stretching regime when such a regime exists). In this case the scaling laws are

$$\frac{L}{t_c} = \left[\frac{2(1+\widetilde{c})}{3\theta} \right]^{1/2} \left(\frac{t}{t_c} \right)^{5/4} \quad \text{gauge,} \tag{4.25}$$

$$\frac{L}{t_c} = \left[\frac{2(1+\widetilde{c})}{3\theta} \right]^{1/2} \left(\frac{t}{t_c} \right)^{5/4} \ln\left(\frac{\lambda}{6}\frac{t}{t_c}\right) \left(\ln\frac{L}{\delta} \right)^{1/2} \quad \text{global,} \tag{4.26}$$

$$v = \left[\frac{3}{\theta(1+\widetilde{c})} \right]^{1/2} \left(\frac{t}{t_c} \right)^{1/4} \quad \text{gauge,} \tag{4.27}$$

$$v = \left[\frac{3}{2\theta(1+\widetilde{c})} \right]^{1/2} \left(\frac{t}{t_c} \right)^{1/4} \ln\left(\frac{\lambda}{6}\frac{t}{t_c}\right) \left(\ln\frac{L}{\delta} \right)^{1/2} \quad \text{global.} \tag{4.28}$$

This is a high-density regime, arising when the correlation length L is close to the friction length—either because it started that way or because it becomes so during a period of $L \propto t^{1/2}$ evolution (recall that in the radiation era the friction length grows as $\ell_f \propto t^{3/2}$).

Although friction still dominates the dynamics, the higher string curvature (and consequently higher velocity) means that the network is now chopping off a considerable amount of energy into loops—in fact, proportionally more than in the final, linear regime. However, note that there is still no small-scale structure (i.e., we still have $k \approx 1$). Therefore this shows that small-scale structure is not the only determining factor for loop production—the long-string density (i.e., L) is just as important. This is the reason why we chose the

form of our loop production ansatz (2.32), explicitly separating the effects of large (through L) and small-scale structure (through the parameter α).

The $L \propto t^{5/4}$ scaling law was previously suggested by Kibble. However, note that the above relations only hold in the radiation era. In the corresponding regime in the matter era for very light strings, we have the scaling laws

$$L \propto t^{3/2}, \quad v \propto t^{1/2}. \tag{4.29}$$

3. Linear regime

This is the well-known ''final'' scaling regime—it is always the end point of cosmological string evolution, arising when the friction lengthscale becomes subdominant with respect to the Hubble length. Assuming that k (as well as $\widetilde{c}$) are constant in each regime, we find the scaling laws

$$L = [k_r(k_r + \widetilde{c}_r)]^{1/2} t \quad \text{radiation,} \tag{4.30}$$

$$L = \left[\frac{9k_m(k_m + \widetilde{c}_m)}{8} \right]^{1/2} t \quad \text{matter,} \tag{4.31}$$

$$v = \left[\frac{k_r}{(k_r + \widetilde{c}_r)} \right]^{1/2} \quad \text{radiation,} \tag{4.32}$$

$$v = \left[\frac{k_m}{2(k_m + \widetilde{c}_m)} \right]^{1/2} \quad \text{matter.} \tag{4.33}$$

Now, the simplest way to proceed is to look for the values of $\widetilde{c}$ and k that match the simulations:

$$\widetilde{c}_r \approx 0.24, \quad k_r \approx 0.18, \tag{4.34}$$

$$\widetilde{c}_m \approx 0.17, \quad k_m \approx 0.49. \tag{4.35}$$

Hence, according to our interpretation of this model, it predicts a larger loop production rate and more small-scale structure in the radiation era (recall that more small-scale structure corresponds to a smaller k)—which is exactly what is seen in numerical simulations [4]. This shows that our interpretation of k as being related to the presence of small-scale structure is at least qualitatively correct. Notice that the scaling parameters are much less sensitive to variations in $\widetilde{c}$ than those of previous analytic models; this will be relevant below.

Furthermore, we can get some feeling for the validity of our ansatz (2.47) for k by finding out which values we obtain with the known values of the ratios $\zeta = L/t$ in the radiation and matter eras [4]. In the first case we have $\zeta_r \sim 0.28, k_r \sim 0.19$ in excellent agreement with Eq. (4.34). In the matter era the scaling value of $\zeta_m \sim 0.535$ also gives good agreement with the simulations, since $k_m = 0.50$ with $\chi = \sqrt{2}$ (the dashed line ansatz in Fig. 1). Note, however, that matter era correspondence is upset if we use the $\chi = 0.57$ ansatz modified to match collapsing circular loops. Nevertheless, these results indicate that the ansatz (2.47), originally justified for string loops, is probably extensible to the long string network, although the point χ where the transition between the constant and linear regimes takes place should be studied in greater detail. If this is indeed the case, then it

appears that this simple model goes a long way towards solving the ''matching'' problem at the matter-radiation transition—previously, a significant failing of the ''one-scale'' model.

Of course, these results are a manifestation of the fact that we require additional degrees of freedom to incorporate small-scale structure satisfactorily (see, for example, Ref. [5]), but perhaps there are fewer required than at first anticipated.

C. Loop scaling laws

We already know how to determine the (relative) loop density at all times; we simply have to evaluate

$$\varrho(t) = g\widetilde{c}L^2(t)\int_{t_c}^{t}\frac{v_\infty(t')}{L^4(t')}\frac{a^3(t')}{a^3(t)}\frac{\ell(t,t')}{\alpha(t')}dt'$$
$$+L^2(t)\frac{a^3(t_c)}{a^3(t)}\int_{L_c}^{L_{\text{cut}}}n_\ell(\ell',t_c)\ell(\ell',t_c)d\ell', \tag{4.36}$$

where $\ell(t,t')$ is the length at time t of loops produced at time t', $\ell(\ell',t_c)$ is the length at time t of a (primordial) loop with length ℓ' at t_c and n_ℓ is the Vachaspati-Vilenkin loop number density distribution. If necessary, we can also analyze the distributions of loop lengths, etc.—although this will not be done in this paper. There is still, however, one point to be discussed—we must propose an *Ansatz* for the parameter α, which should be related to the presence of string small-scale structure.

We know on physical grounds that $\alpha \sim 1$ in the friction dominated epoch, since strings are nonrelativistic and any wiggles are quickly erased; this conclusion is also supported qualitatively by observing the actual evolution of networks in quenched liquid crystals [12]. On the other hand, all studies of radiative backreaction lead us to expect α to be a constant (significantly less than unity) in the linear scaling regime. For example, in the case of a gauge GUT string network numerical simulations [4] show that $\alpha_{\text{GUT}} < 5 \times 10^{-3}$ (note that our definition of α differs from that in the numerical simulation papers—where it is defined as ℓ/t). We will, therefore, use the simple Ansatz

$$\alpha(t) = \frac{1+\alpha_{\text{sc}}t/t_*}{1+t/t_*}, \tag{4.37}$$

where α_{sc} is the constant scaling value. Note that this is such that in the transition between the damped and free regimes the physical loop length at formation ($\ell = \alpha L$) is constant. In this simple way we can ''phenomenologically'' account for the build-up of small-scale structure as seen in the numerical simulations [4]. In particular, for the case of GUT strings, this build-up takes about 4 orders of magnitude in time, in agreement with a result obtained by Allen and Caldwell and by Austin [6] by estimates of the evolution of the linear kink density in a ''one-scale'' model context.

Although Eq. (4.36) cannot be evaluated analytically in general due to the complicated behavior of the integrands (and in particular of the ℓ factors), it is possible (under some simplifying assumptions) to obtain an analytic solution in the linear regime. For simplicity we will neglect the loops existing at the start of this regime, $t=t_s$. Since loops are much smaller than the horizon, we can approximately neglect the effect of expansion; furthermore, we can also assume that the loop velocity is close to the terminal velocity, $v_\ell \sim 1/\sqrt{2}$, so that we approximate $\Gamma' v^6 \sim \Gamma$. These two simplifying assumptions mean that our calculation will be a slight underestimate of the true loop density. The loop decay function in this case is

$$\ell(t,t') = \ell' - \Gamma G\mu(t-t'), \quad t' \leq t \leq t' + \frac{\ell'}{\Gamma G\mu} \tag{4.38}$$

$$\ell(t,t') = 0 \quad \text{otherwise,} \tag{4.39}$$

with the initial loop length being

$$\ell' = \alpha_{\text{sc}}\zeta t', \tag{4.40}$$

and we used $\zeta = L/t$. Note that the coefficient $\Gamma G\mu$ will be altered if the preferred loop decay channel is not gravitational radiation, but Goldstone bosons or electromagnetic radiation. With these assumptions, Eq. (4.36) reduces to

$$\varrho(t) = \frac{g\widetilde{c}v_\infty}{\alpha_{\text{sc}}\zeta^2}t^2\int_{f(t)}^{t}\frac{\ell(t,t')}{t'^4}\frac{a^3(t')}{a^3(t)}dt', \tag{4.41}$$

where

$$f(t) = t_s, \quad t \leq \frac{t_s}{\xi}, \tag{4.42}$$

$$f(t) = \xi t, \quad t \geq \frac{t_s}{\xi}, \tag{4.43}$$

and

$$\frac{1}{\xi} = 1 + \frac{\alpha_{\text{sc}}\zeta}{\Gamma G\mu}. \tag{4.44}$$

The path of integration for all times is schematically represented in Fig. 8. The integral can be therefore conveniently split into two cases, the transition point corresponding to the moment of the decay of the loops formed at t_s. Then one finds the late-time solutions

$$\frac{\rho_0(t)}{\rho_\infty(t)} = \frac{g\widetilde{c}v_\infty}{\alpha_{\text{sc}}\zeta^2}[2(\zeta\alpha_{sc}+\Gamma G\mu)(\xi^{-1/2}-1)$$
$$-\tfrac{2}{3}\Gamma G\mu(\xi^{-3/2}-1)] \quad \text{radiation,} \tag{4.45}$$

$$\frac{\rho_0(t)}{\rho_\infty(t)} = \frac{g\widetilde{c}v_\infty}{\alpha_{\text{sc}}\zeta^2}[(\zeta\alpha_{\text{sc}}+\Gamma G\mu)\ln\xi^{-1}$$
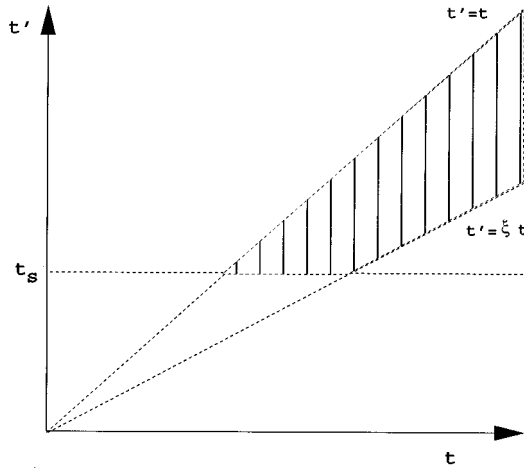$$-\Gamma G\mu(\xi^{-1}-1)] \quad \text{matter.} \tag{4.46}$$

FIG. 8. The interval in t' giving a nonzero loop length contribution to the loop density integral Eq. (4.41) for different times t.

Again, this can be confirmed numerically (see Sec. V). Figure 9 depicts a typical situation; after an initial build-up while no loops have decayed, we reach a constant ratio. Note that Eqs. (4.45) and (4.46) should be testable against numerical simulations. With the values of $\widetilde{c}$ and k quoted above and assuming that $\alpha_{sc} = 10^{-3}$ and $\Gamma G\mu = 65 \times 10^{-6}$ this model predicts the scaling density ratios to be

$$\frac{\rho_0(t)}{\rho_\infty(t)} = 0.59 \quad \text{radiation,} \qquad (4.47)$$

$$\frac{\rho_0(t)}{\rho_\infty(t)} = 0.19 \quad \text{matter.} \qquad (4.48)$$
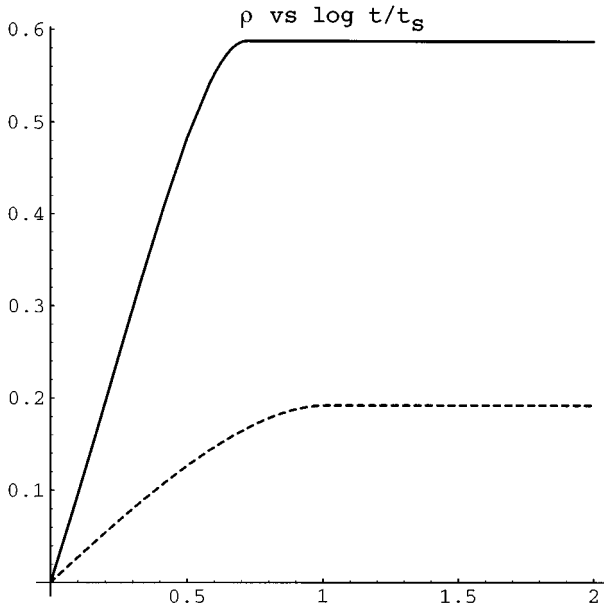
FIG. 9. Analytical estimate of the evolution of the ratio of the loop and long string energy densities in the linear scaling regime, for $\alpha_{sc} = 10^{-3}$ and $\Gamma G\mu = 65 \times 10^{-6}$, in the radiation (solid) and matter (dashed) eras. Time is in orders of magnitude from the start of the regime. The logarithm is to base 10.
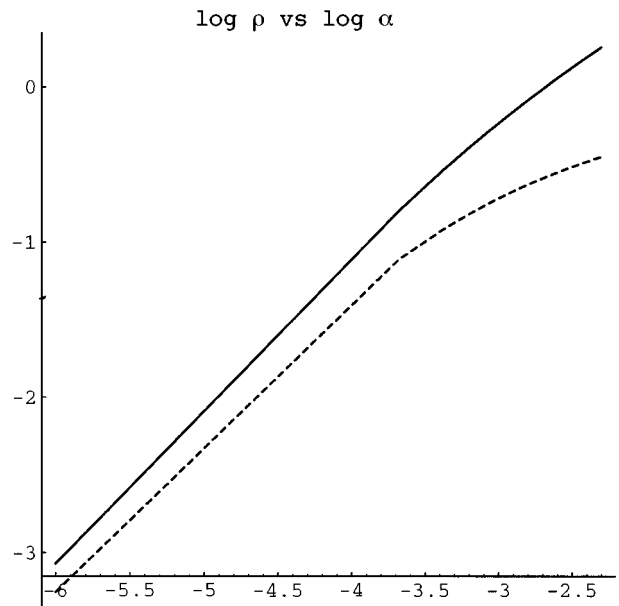

FIG. 10. Expected ratios of the loop and long string densities in the linear scaling regime, in the radiation (solid) and matter (dashed) eras for gauge GUT strings, in terms of the small-scale structure parameter α_{sc} and with $\Gamma G\mu = 65 \times 10^{-6}$. The logarithm is to base 10.

Notice that it is possible (at least in principle) to measure both α and the ratio of the densities from numerical simulations (Γ can also be estimated in this way). Hence the prediction of this model for the density ratio in the scaling regime Eqs. (4.45) and (4.46) and even the approach to it can be tested numerically. Figure 10 shows the predicted ratios for gauge GUT strings in the radiation and matter eras, at fixed $\Gamma G\mu$ for all possible values of α_{sc} (the upper limit is inferred from numerical simulations, the lower limit assumed on physical grounds). Note that if loops are large enough at formation, then in the radiation era their scaling density can be dominant (by a factor of up to two—but recall that this analytic calculation underestimates the loop density). In the matter era, the energy density in loops can be at most 35% of that in long strings.

Finally, let us just briefly mention two other helpful quantities in characterizing the evolution of a cosmic string network. The first is the fraction of the energy density in long strings at a time t which is converted into loops within the next Hubble time; this is given by

$$f_H = g \frac{\widetilde{c}}{H} \frac{v_\infty}{L}, \qquad (4.49)$$

and the limiting values for GUT strings in the radiation and matter eras are respectively

$$f_H \sim 0.81 \quad \text{radiation era,} \quad f_H \sim 0.18 \quad \text{matter era.} \qquad (4.50)$$

The second is the number of loops chopped off by the long string network per Hubble volume per Hubble time, given by

TABLE I. Some relevant scales for the evolution of the four cosmologically interesting string networks.

Properties	Gauge EW	Global Ax.	Global GUT	Gauge GUT
T_c/GeV	10^2	10^{10}	10^{15}	10^{16}
$G\mu$	10^{-34}	10^{-18}	10^{-8}	10^{-6}
λ	Irrelevant	0.2	0.2	Irrelevant
θ	2×10^{15}	1×10^8	1×10^3	29
t_c/t_{Pl}	4×10^{32}	3×10^{16}	3×10^6	3×10^4
t_i/t_c	1	60	60	1
$t_\star/t_c$	7×10^{25}	2×10^8	351	855

TABLE II. Initial conditions on the ratio of the length scale to the horizon, $(L/t)_i$, to be used in the figures and discussion below.

Case	Gauge EW	Global Ax.	Global GUT	Gauge GUT
Solid	10^{-1}	0.9	0.9	0.9
Dashed	10^{-4}	5×10^{-2}	0.2	0.2
Dotted	10^{-8}	10^{-3}	0.02	0.05

$$n = g\,\frac{\widetilde{c}}{\alpha}\,\frac{v_\infty}{H^4 L^4}, \tag{4.51}$$

with asymptotic values

$$n \sim 2.2\times10^5 \quad \text{radiation era,} \quad n\sim4.5\times10^3 \quad \text{matter era.} \tag{4.52}$$

These quantities should also be measurable in numerical simulations.

V. THE COSMOLOGICALLY RELEVANT NETWORKS

A. Introduction

We can now discuss the four cosmologically interesting cases: gauge electroweak and GUT, and global axionic and GUT strings. To summarize the cases to be studied numeri-

cally, some relevant quantities in each case are listed in Table I. The initial conditions taken for the correlation length (expressed in terms of the ratio L/t) are summarized in Table II. Note that the initial condition on velocity is not independent—see (4.19) in Sec. IV.

There is another parameter that we must estimate, namely the typical loop size at formation in the linear scaling regime, α_{sc}. As we have seen in the above discussion, this is crucial in determining the ratio of the energy densities in loops and long strings. We will assume that $\alpha_{\text{sc}} \sim G\mu$.

B. Electroweak and axionic strings

We start by noting that for electroweak and axionic strings we cannot meaningfully treat the case of very high string density (that is, the case where L is initially close to the friction lengthscale). This is because in this case loop reconnections onto the string network may have a significant effect. In all other situations the effect of such reconnections can be neglected.

For gauge electroweak strings (see Figs. 11 and 12) the epoch of friction-dominated dynamics ends well into the
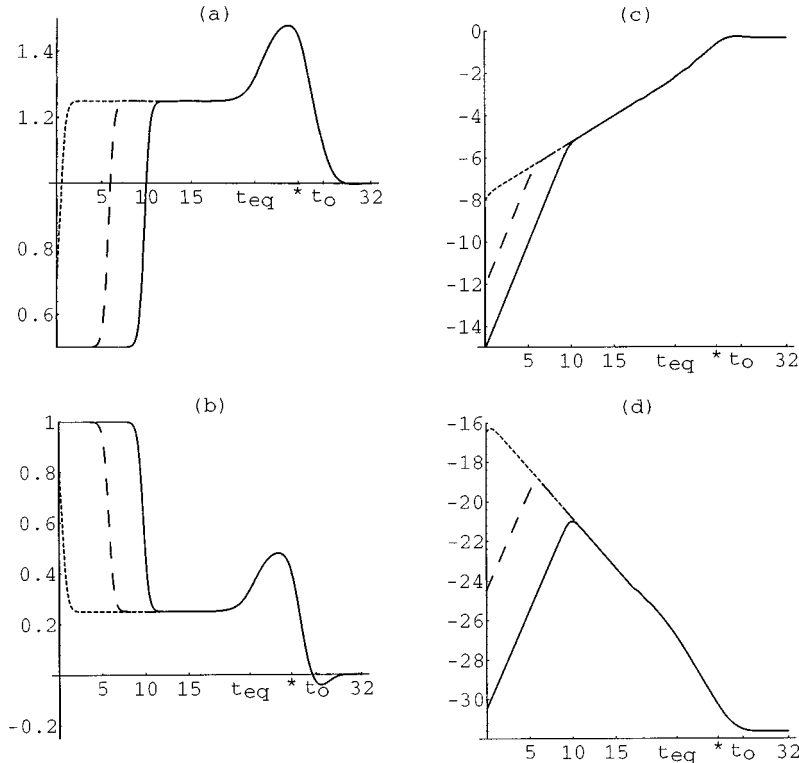

FIG. 11. The complete evolution of an electroweak gauge long-string network. Plots successively represent the exponents of the power-law dependence of L (a) and v (b), log v (c), and the log of the ratio of the long string and background densities (d). The horizontal axis is labeled in orders of magnitude in time from the moment of string formation, and initial conditions are specified in Table II.
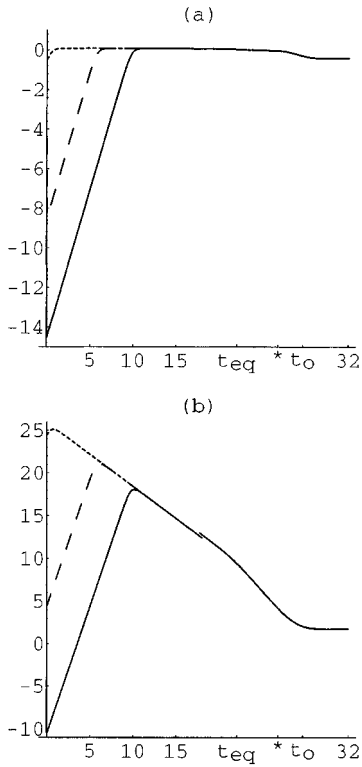
FIG. 12. Characteristics of loop production by electroweak strings: log plots of the fraction of the energy density going into loops per Hubble time (a) and of the number of loops produced per Hubble volume per Hubble time (b). The horizontal axis is labeled in orders of magnitude in time from the moment of string formation, and initial conditions are specified in Table II; we have taken $\alpha_{\rm sc} \sim 10^{-31}$ and $\Gamma G\mu \sim 10^{-30}$.

matter era. One of the most important results on this paper is that the early-time evolution of the network depends crucially on the initial string density. Note that among other things this depends on the order of the phase transition at which the strings form. If this density is low, strings have very small velocities and according to our previous discussion the network starts evolving in the stretching regime, which can last up to ten orders of magnitude in time. In this regime, the energy transfer into loops is negligible; this can be seen in Fig. 12(b), where initially less than one loop is produced per Hubble time.

As the string velocity increases, energy losses to loop production become more and more important and eventually the network "switches" rather quickly to the Kibble regime. Here, the fraction of the energy density in long strings that is transferred into loops per Hubble time is in fact larger than unity. Of course there is nothing unphysical about this, since the string network also gains energy during the time interval in question due to stretching—most of which is immediately converted into loops. Note that in this regime, although the fraction of transferred energy is constant, the number of loops produced per Hubble volume per Hubble time decreases: this is because the correlation length is "catching up" with the horizon, so larger and larger loops (relative to the horizon) are produced, given our assumption that during the friction-dominated epoch $\alpha \approx 1$.

In the opposite regime for high initial densities, the initial velocity is much larger, so loop formation is important right from the start and the Kibble regime begins immediately. Note that the first few orders of magnitude in time after the formation of an electroweak string network are the relevant period for baryogenesis mechanisms; we therefore believe that these results can shed some new light in this area.

As we approach $t_{\rm eq}$, the network scaling switches again to a different regime, though now rather more slowly. This would be the matter-era analogous of the Kibble regime ($L \propto t^{3/2}$, $v \propto t^{1/2}$), except that it is not particularly distinct given that the friction-dominated dynamics ends and the network evolves towards the final linear scaling regime. As we have already pointed out, the long-string network reaches the linear scaling regime about today. Nevertheless, it is still building up small-scale structure and, if our *Ansatz* is valid, it will keep on doing so for another 20 orders of magnitude in time if gravitational radiation is the dominant decay mechanism (electromagnetic losses would intervene first for superconducting strings).

It should be noted that although string dynamics is friction-dominated until $t_\star$, the same is not true for the corresponding term in the evolution equation for L Eq. (2.23) (this is of course due to the v^2 dependence of that term). In fact the expansion term in Eq. (2.23) is always dominant, although in the Kibble regime the friction and loop production terms are of the same order of magnitude. Also note that, as we said before, the loop formation term is proportionally more important in the Kibble regime than in the "free" scaling regime—in fact, the (linear-log) plot of the ratio of the friction and expansion terms in Eq. (2.23) is indistinguishable (apart from the scale of the y axis) from Fig. 11(a).

Axionic and GUT strings reach the final scaling regime well before $t_{\rm eq}$, so we will separately consider the approach to scaling in each case and then the transition between the linear scaling regimes in the radiation and matter eras.

Figures 13 and 14 depict the approach to scaling of an axionic string network. The discussion is analogous to the one for the early evolutionary stages of electroweak strings, except for the different orders of magnitude involved. The other difference is of course that the additional logarithmic dependencies affect all the transient scaling laws with the exception of $L \propto t^{1/2}$. Note that in all cases the effect of the logarithms is to increase the exponent of the power-law dependencies. The stretching regime can now last up to five orders of magnitude in time.

C. Global and gauge GUT strings

The approach to scaling for a global GUT string network is shown in Fig. 15; as we mentioned previously, in this case loop reconnections onto the network are not important and hence the cases plotted are representative of all physically meaningful initial conditions. In this case the period of friction-dominated evolution is much shorter, and so the stretching and Kibble regimes, although still clearly distinguishable, are not very definite. Again, the effect of the logarithmic corrections for global strings is to increase the power-law dependencies. It takes a global GUT string network about six orders of magnitude in time to reach the scaling regime.
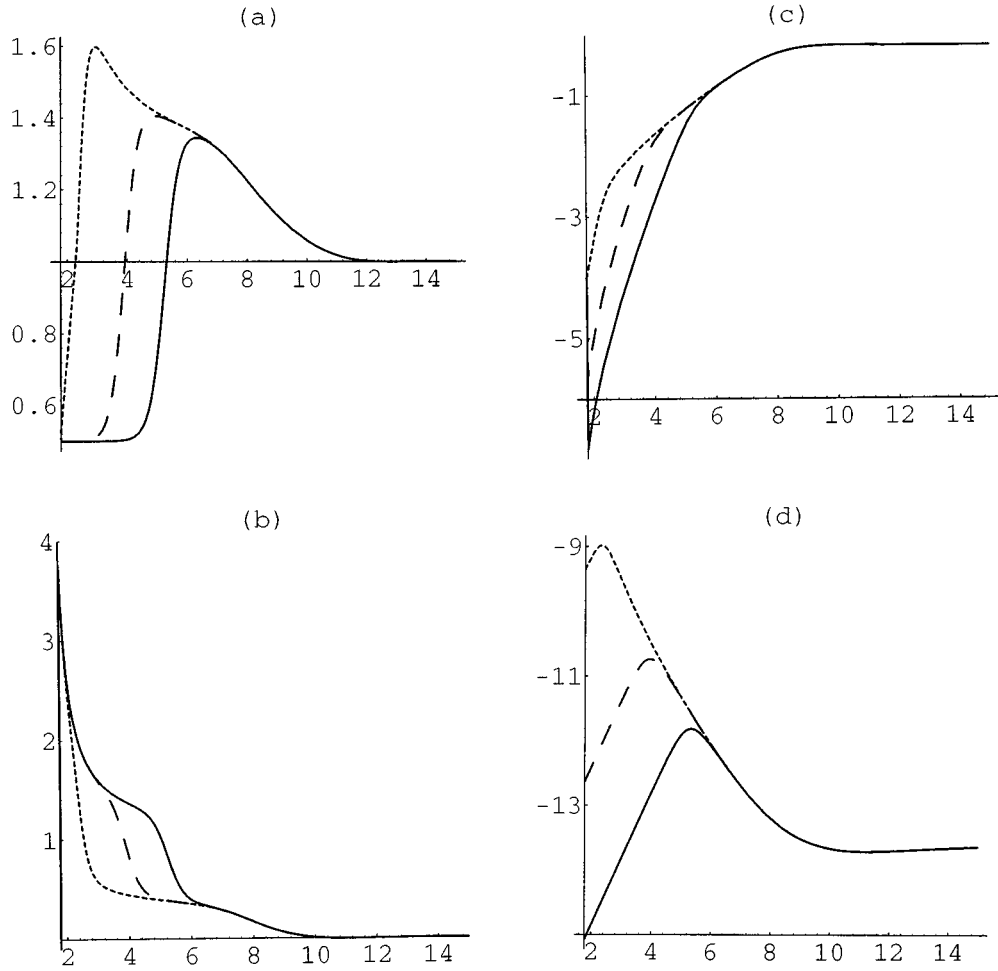
FIG. 13. The approach to scaling for an axionic long-string network. Plots successively represent the exponents of the power-law dependence of L and v, v itself, and the ratio of the long string and background densities. The horizontal axis is labeled in orders of magnitude in time from the moment of string formation, and (c) and (d) are log plots; initial conditions are specified in Table II.

Now, let us concentrate on the more interesting case of gauge GUT strings for which the approach to the linear regime is shown in Figs. 16 and 17. Here the epoch when friction dominates the dynamics lasts less than three orders of magnitude in time, and the linear regime is reached about six orders of magnitude after string formation. Hence the linear scaling regime is approached faster than previously estimated and, more importantly, strings become relativistic at a very early epoch. Consequently, energy losses to loops are relevant at all times (see Fig. 17). One should also notice the similarity between the plots of the exponent of the power-law dependence of the length scale L [labeled (a) in 16] and of the fraction of the energy density in the form of long strings converted into loops per Hubble time [labeled (a) in 17]. This is evidence of the fact that loop formation is the crucial mechanism for cosmological string network evolution. It should be emphasized that with our ansatz for α, $\alpha_{sc} \sim 10^{-3}$ and $\Gamma G \mu \sim 65 \times 10^{-6}$ it takes about 4 orders of magnitude in time for α to evolve from $\alpha=1$ to $\alpha=\alpha_{sc}$, and during this time the physical size of the loops formed changes by less than a factor of 3. This is in agreement with both simulations [4] and previous analytical estimates [6].

For the given parameters in the radiation era linear scaling regime, the ratio of the energy densities in loops and long

strings is $\varrho_{num} \approx 0.74$ [see Fig. 17(c)]; recall that our analytical estimate was $\varrho_{est} \sim 0.59$. This 20% discrepancy is explained by the fact that in the analytic estimate we have assumed that loops always have $v_\angle = 1/\sqrt{2}$, while numerically we assume that their initial velocity is that of the long string network at the moment of formation. Furthermore, while with our simplifying assumptions one finds that in the radiation-era scaling regime loops decay at a time $t_{decay} \sim 5.18 t_f$ after formation, the exact result is $t_{decay} \approx 6.22 t_f$. For comparison, note that the original "one-scale" model predicts $\varrho_{one} \sim 2.36$, a considerable overestimate.

However, the maximum value of ϱ is $\varrho_m \sim 23.5$ and it occurs before the linear scaling regime is reached, at a time $t_m \sim 10^{5.4} t_c$. At this time the ratio of the loop and background densities also reaches its maximum,

$$\left(\frac{\rho_o}{\rho_b} \right)_{t_m} \sim 1.2 \times 10^{-2}. \qquad (5.1)$$

Note that although less loops are produced in the friction-dominated regime, they are bigger than the ones in the linear regime (since $\alpha \sim 1$) and hence live much longer. Conse-
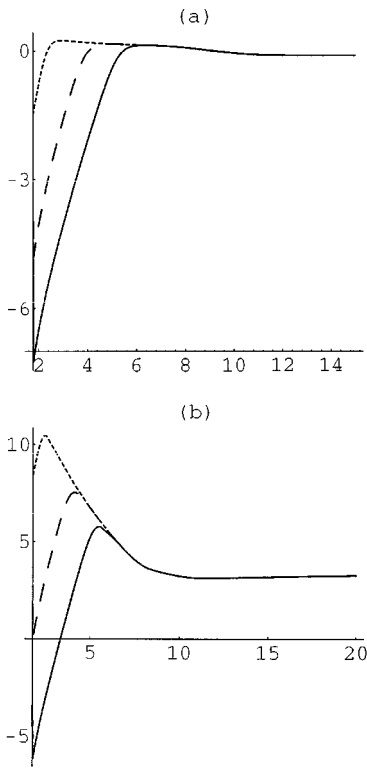
FIG. 14. Loop production during the approach to scaling of an axionic string network. The horizontal axis is labeled in orders of magnitude in time from the moment of string formation, and plots represent the log of the fraction of the energy in long strings converted into loops per Hubble time (a) and the log of the number of loops created per Hubble volume per Hubble time (b). We have taken $\alpha_{sc} \sim q$ [see Eq. (2.31)].

quently, ϱ_{dyn} always increases in the friction-dominated epoch. Interestingly, we find that the above numerical results are independent of both the initial conditions and the loop size at formation α (which at t_m is already less than unity). This epoch will therefore be important for mechanisms such as string-induced electroweak baryogenesis.

Furthermore, we have numerically investigated the dependence of these results on the string mass μ. The result is that the maximum values of the above ratios are

$$\text{Max}\varrho \sim 2 \times 10^{-2} (G\mu)^{-1/2}, \tag{5.2}$$

$$\text{Max}\left(\frac{\rho_o}{\rho_b}\right) \sim 10(G\mu)^{1/2}. \tag{5.3}$$

Hence, as we decrease the string mass there is proportionally more energy density in loops than in long strings, but the total string density decreases with respect to the background density. Note that this completes the demonstration of the statement that cosmic strings can never dominate the energy density of the universe. We shall discuss this in greater detail in a future publication.

Finally, we discuss the transition between the radiation and matter era linear scaling regimes (see Figs. 18–20). Using our ansatzes for k and α, and assuming a smooth change of $\tilde{c}$ (although this is strictly not necessary given the relatively weak dependence of the scaling properties on $\tilde{c}$) we

can match all results the from numerical simulations [4] and our own analytical estimates (see Sec. IV C) with an error of less than 10%. This is a significant achievement given the fact that in previous analytic models the discrepancies were typically of order 100%.

Note that this is a much slower and smoother process than previously estimated, extending for about eight orders of magnitude in time. This is the reason why Bennett and Bouchet, [4] having studied this transition with a series of numerical simulations covering a range of five orders of magnitude in time, do not see the scaling parameters "going flat." In fact, one can say that the string network never leaves the scaling regime—the exponent of the power-law dependence of L is never more than ten percent away from the scaling value. It is also interesting to observe that the string velocity increases just after t_{eq}, before it decreases to the matter-era scaling value [see Fig. 18(d)]; this is due to the comparatively rapid change in the expansion rate.

As for the matter era ratio of the energy densities in loops and long strings, we get the numerical result $\varrho_{num} \approx 0.27$ [see Fig. 20(c)], while our analytical estimate was $\varrho_{est} \sim 0.19$. The discrepancy has now increased to 30%, which is of course expected since the long string velocity is now smaller (so $v_\ell = 1/\sqrt{2}$ is a poorer approximation). In this case, the original "one-scale" model severely underestimates this ratio, predicting $\varrho_{one} \sim 0.01$. Finally, note the effect of the logarithmic corrections for global strings in the evolution of the ratio of the long string and background energy densities (see Fig. 19).

To conclude, it should be emphasized that this quantitative picture of GUT string evolution can lead to important modifications in the structure formation scenarios involving cosmic strings.

VI. CONCLUSIONS

In this paper we have presented a detailed account of a recently-developed generalized "one-scale" model of string network evolution [8,16] where a characteristic lengthscale (the "correlation length" or average interstring distance in the case of long strings, the physical loop length in the case of loops) and the average velocity are the dynamical variables.

The immediate benefit of this generalization is that one is thus able to properly describe string motion in friction-dominated contexts. As a consequence, this simple model is the first complete and fully quantitative study of the evolution of a string network and the corresponding loop population in both condensed matter (see [16]) and cosmological contexts.

Notably, we established the validity of Kibble's scaling law for intermediate and light energy scale cosmic strings; furthermore, if the initial string density is sufficiently low, there can also be an earlier period during which the strings are conformally stretched. However, despite the relative growth in the string energy ρ_{string}/ρ_b in the damped epoch, we showed that strings can never dominate the energy density of the universe. The model also predicts that electroweak strings are only approaching the linear scaling regime today, whereas GUT strings reach this scaling regime faster than previously estimated. Finally, we have shown that the tran-
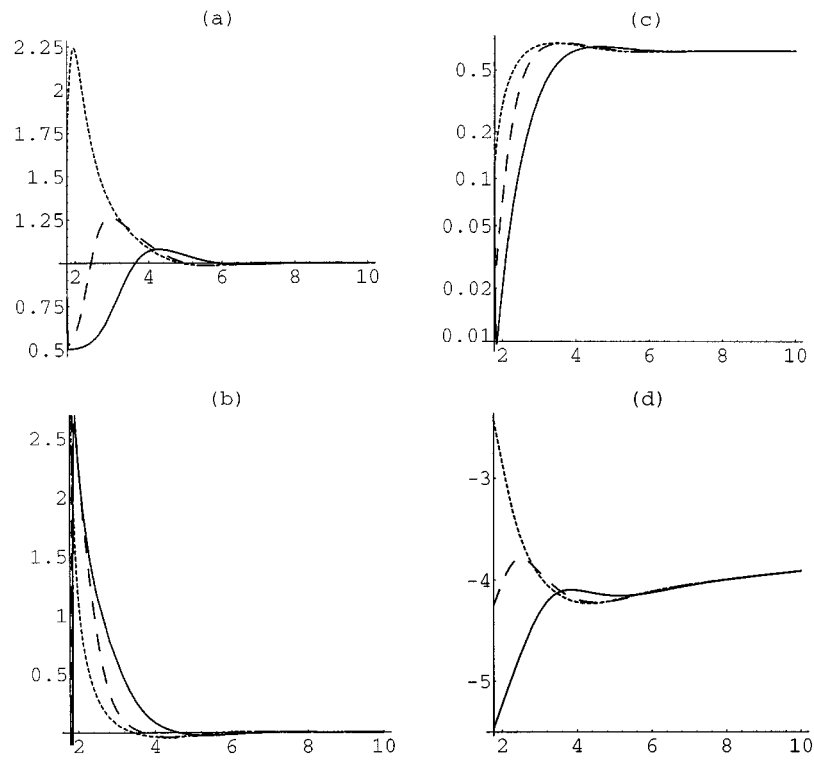
FIG. 15. The approach to scaling of a global GUT string network. Plots successively represent the exponents of the power-law dependence of L (a) and v (b), v itself (c), and the log of the ratio of the long string and background densities (d). The horizontal axis is labeled in orders of magnitude in time from the moment of string formation, and initial conditions are specified in Table II.
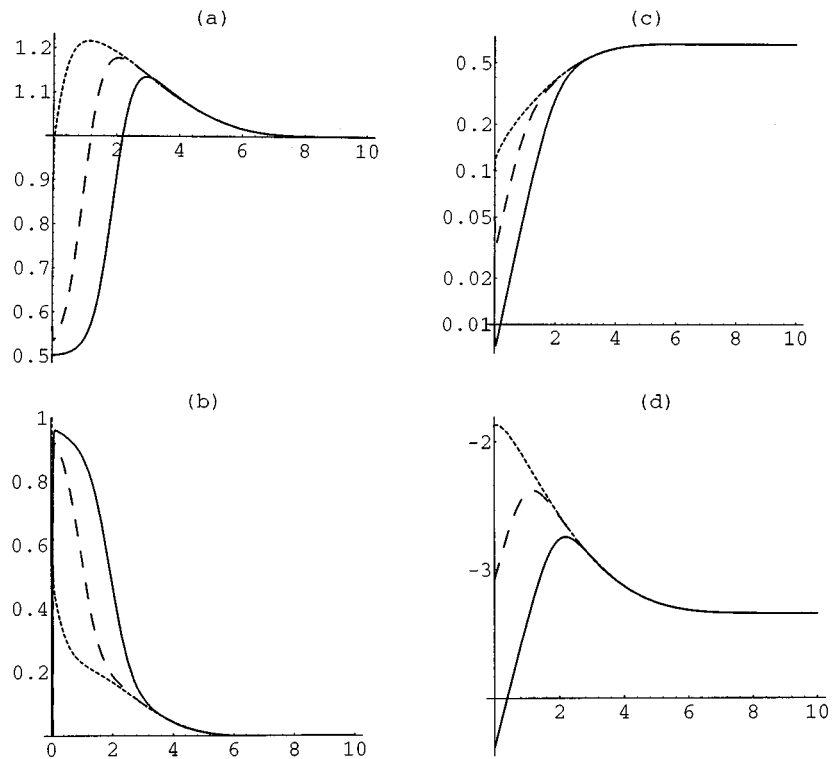

FIG. 16. The approach to scaling of a gauge GUT string network. Plots successively represent the exponents of the power-law dependence of L (a) and v (b), v itself (c), and the log of the ratio of the long string and background densities (d). The horizontal axis is labeled in orders of magnitude in time from the moment of string formation, and initial conditions are specified in Table II.
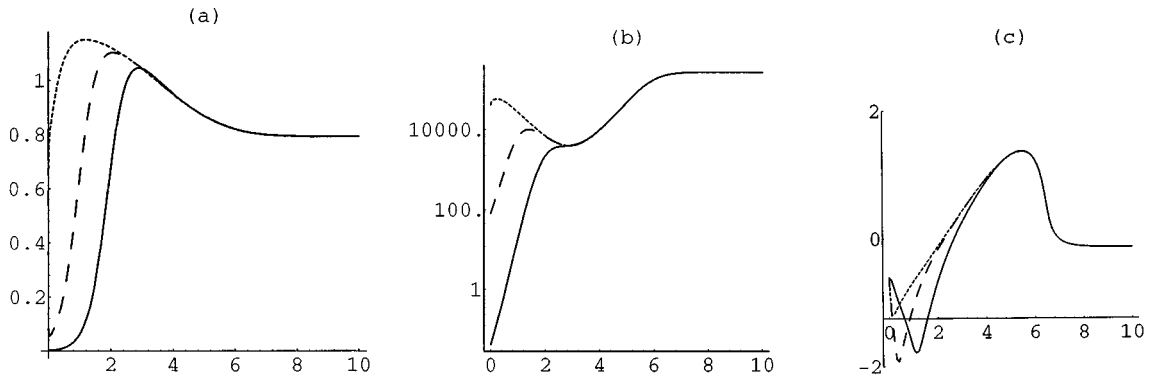
FIG. 17. Evolution of the loop population for a gauge GUT string network. Plots successively represent the fraction of the energy in long strings converted into loops per Hubble time (a), the number of loops created per Hubble volume per Hubble time (b), and the log of the ratio of loop and long string densities (c). Note that (a,b) were obtained from our analytical estimates (see Sec. IV C) while (c) is the (exact) numerical solution of Eq. (4.41). The horizontal axis is labeled in orders of magnitude in time from the moment of string formation, and we have taken $\alpha_{sc} \sim 10^{-3}$ and $\Gamma G \mu \sim 65 \times 10^{-6}$.

sition between the radiation and matter era linear scaling regimes is a very slow process.

Application of the model to string loops has also led to the determination of the evolution of the density and other relevant properties of the loop population. We can use this model to determine the loop density and other relevant properties at all times. We have found that for typical values of the parameters characterizing loop production and decay there is more energy density in loops than in long strings.

These results can significantly affect some cosmological string scenarios. The insight gained on the friction-

dominated epoch of string evolution also calls for a re-examination of the vorton problem [25] and of string-induced baryogenesis [26]. It should also be possible to obtain more accurate estimates of the contribution of axions to dark matter, and, of course, our results on the radiation-matter transition for GUT strings can affect structure formation scenarios. We hope to tackle some of these problems in the very near future.

We have also pointed out that the study of the evolution of cosmic string networks has been an effort involving both analytic and numerical work. Our results concerning the
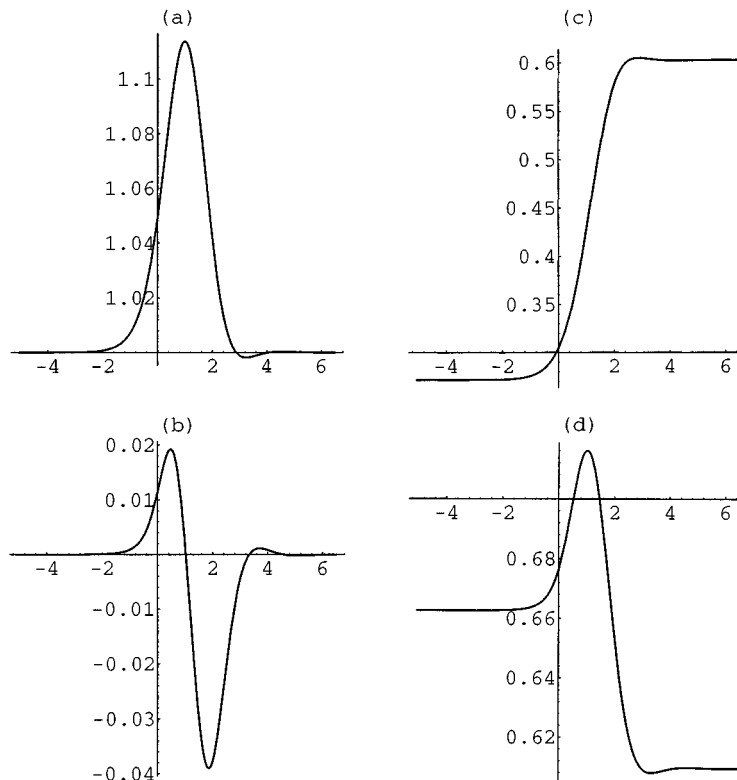

FIG. 18. Evolution of GUT long-string networks (both gauge and global) in the transition between the radiation and matter linear scaling regimes. Plots respectively represent the exponent of the power-law dependence of L (a) and v (b), the ratio L/t (c), and velocity (d). The horizontal axis is labeled in terms of the logarithm of the scale factor [with $a(t_{eq}) = 1$]; it spans the period between $10^{-10} t_{eq}$ and $10^{10} t_{eq}$.
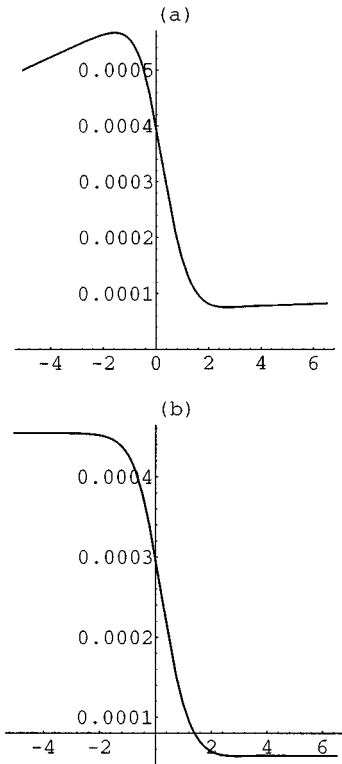
FIG. 19. Evolution of the ratio of long string and background densities for global (a) and gauge (b) GUT string networks in the transition between the radiation and matter eras. The horizontal axis is labeled in terms of the logarithm of the scale factor [with $a(t_{eq})=1$]; it spans the period between $10^{-10}t_{eq}$ and $10^{10}t_{eq}$.
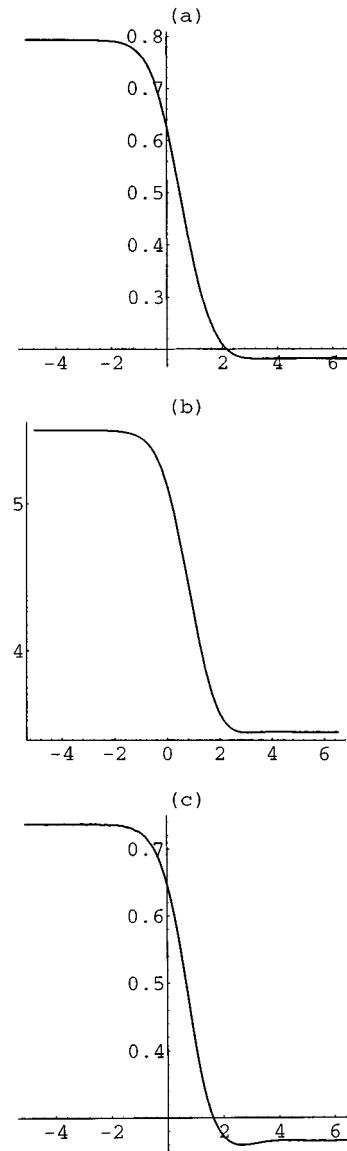

FIG. 20. Evolution of loop characteristics for gauge GUT string networks in the transition between the radiation and matter eras. Plots represent the fraction of the energy density in long string converted into loops per Hubble time (a), the log of the number of loops produced per Hubble volume per Hubble time (b), and the ratio of the energy densities in loops and long strings (c). The horizontal axis is labeled in terms of the logarithm of the scale factor [with $a(t_{eq})=1$]; it spans the period between $10^{-10}t_{eq}$ and $10^{10}t_{eq}$; we have taken $\alpha_{sc}\sim 10^{-3}$ and $\Gamma G\mu\sim 65\times 10^{-6}$.

friction-dominated epoch of string evolution make it clear that a numerical study of this epoch is long overdue, not least because (as was pointed out by Vilenkin [18]) including the frictional force is simplicity itself: it amounts to a redefinition of the Hubble parameter, as can be seen from Eqs. (2.12) and (2.13). There is also a need for a more careful study of the loop population. We have made several predictions regarding the scaling ratios of the loop and long string densities as a function of parameters characterizing the loop production and decay; these should be testable by (slightly modified) existing numerical simulations.

Apart from the effect of reconnections back onto the long string network, which is non-negligible in some cases, the outstanding remaining problem is that of the small-scale structure seen in the simulations [4]. We believe that the parameter k, defined in Eq. (2.44), will ultimately provide a phenomenological means of introducing small-scale structure effects in this model. Some steps in that direction have already been taken in this essay—in particular, a possible solution for the famous ''matching'' problem of Kibble's one-scale model has already become apparent. In particular, it seems likely that we can relate k to the effective (''renormalized'') string energy per unit length $\tilde{\mu}$, which is numerically seen to provide a good description of small-scale structure. These important issues are presently being considered.

[1] T.W.B. Kibble, Nucl. Phys. **B252**, 227 (1985); **B261**, 750 (1986).

[2] D.P. Bennett, Phys. Rev. D **33**, 872 (1986); **34**, 3592 (1986).

[3] T.W.B. Kibble, Phys. Rev. D **33**, 328 (1986).

[4] D.P. Bennett and F.R. Bouchet, Phys. Rev. D **41**, 2408 (1990); B. Allen and E.P.S. Shellard, Phys. Rev. Lett. **64**, 119 (1990).

[5] D. Austin, E.J. Copeland, and T.W.B. Kibble, Phys. Rev. D **48**, 5594 (1993).

[6] B. Allen and R.R. Caldwell, Phys. Rev. D **43**, 2457 (1991).

[7] D. Austin, Phys. Rev. D **48**, 3422 (1993).

[8] C.J.A.P. Martins and E.P.S. Shellard, Phys. Rev. D **53**, 575 (1996).

[9] A. Albrecht and N. Turok, Phys. Rev. D **40**, 973 (1989).

[10] D. Mermin, Rev. Mod. Phys. **51**, 591 (1979).

[11] P. de Gennes, *The Physics of Liquid Crystals* (Clarendon, Oxford, 1981); M. Bowick *et al.*, Science **263**, 947 (1994).

[12] I. Chuang *et al.*, Science **251**, 1336 (1991).

[13] M. Salomaa and G. Volovik, Rev. Mod. Phys. **59**, 533 (1987); U. Parts *et al.*, Phys. Rev. Lett. **75**, 3320 (1995).

[14] W.H. Zurek, Nature (London) **317**, 505 (1985); P.C. Hendry *et al.*, *ibid.* **368**, 315 (1994).

[15] A. Abrikosov, Sov. Phys. JETP **5**, 1174 (1957).

[16] C.J.A.P. Martins and E.P.S. Shellard (unpublished).

[17] R.L. Davis and E.P.S. Shellard, Phys. Rev. Lett. **63**, 2021 (1989).

[18] A. Vilenkin, Phys. Rev. D **43**, 1060 (1991).

[19] R. Rohm, Ph.D. thesis, Princeton University, 1985; P. de Sousa Gerbert and R. Jackiw, Commun. Math. Phys. **124**, 229 (1988); M.G. Alford and F. Wilczek, Phys. Rev. Lett. **62**, 1071 (1989).

[20] A.E. Everett, Phys. Rev. D **24**, 858 (1981); W.B. Perkins *et al.*, Nucl. Phys. **B353**, 237 (1991).

[21] N. Turok and P. Bhattacharjee, Rev. Mod. Phys. **61**, 1 (1989).

[22] T. Vachaspati and A. Vilenkin, Phys. Rev. D **30**, 2036 (1984).

[23] J. Garriga and M. Sakellariadou, Phys. Rev. D **48**, 250 (1993).

[24] M.B. Hindmarsh and T.W.B. Kibble, Rep. Prog. Phys. **58**, 477 (1995).

[25] R.L. Davis and E.P.S. Shellard, Nucl. Phys. **B249**, 557 (1989).

[26] R.H. Brandenberger, A.C. Davis, and M. Trodden, Phys. Lett. B **335**, 123 (1994).